CHAPTER 2

Review of literature on microbial farnesene production and its applications*

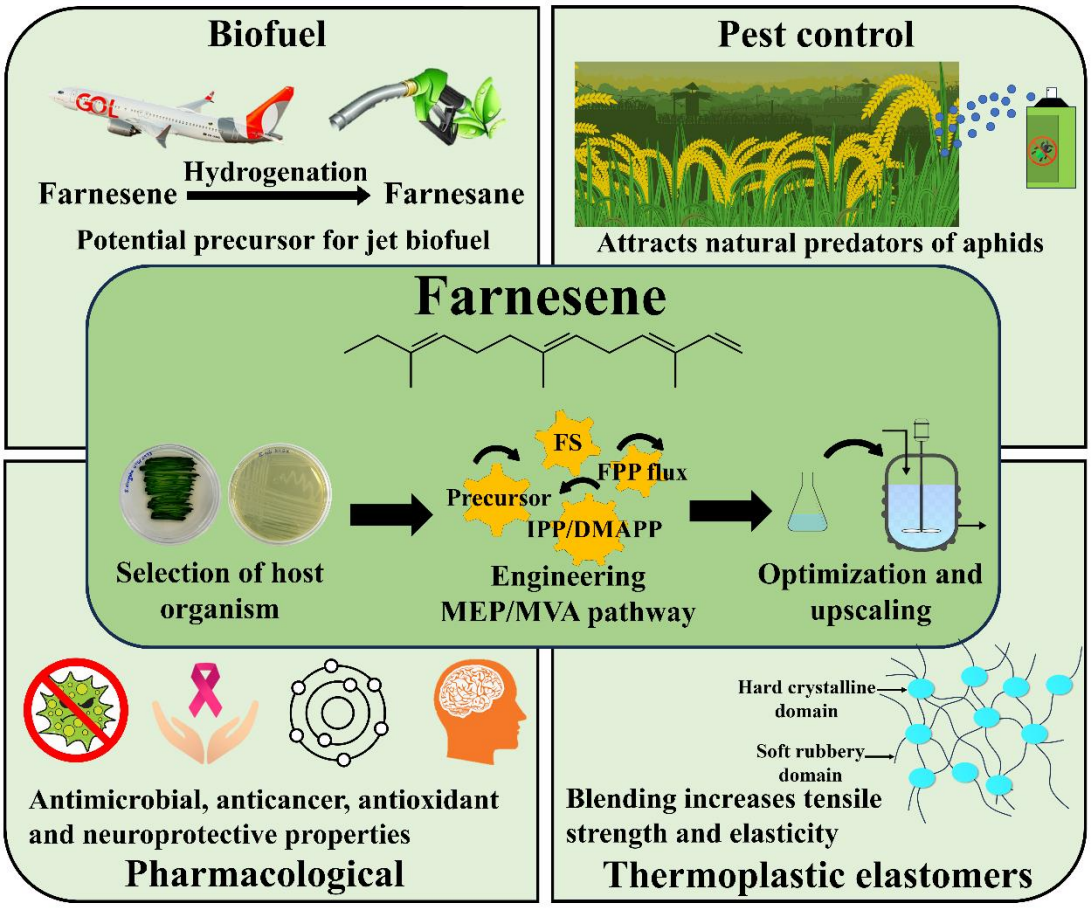

* Part of the work is published in **Akhil Rautela** et al. (2024) A comprehensive review on engineered microbial production of farnesene for versatile applications. 12, 112398. Journal of Environmental Chemical Engineering.

Farnesene (3,7,11-trimethyldodeca-1,3,6,10-tetraene) is a linear sesquiterpenoid synthesized in plants. It is a hydrocarbon formed by three isoprenoid units and has four stereoisomers and two positional isomers (Fig. 2.1). Farnesene, which was initially identified in significant quantities in apple peel, has been recognized for its involvement in the defence mechanisms of plants (Huelin and Murray, 1966; Yang et al., 2016). The characteristic odour of apple fruit is due to α-farnesene and is therefore used as a flavoring agent (Chun-Ping et al., 2015; Cooper et al., 2020). Later farnesene was found to be produced by several plants and is an important component of the plant's essential oil (Usha et al., 2017; Kiyama, 2020; Tian et al., 2022). These essential oils have antiseptic, anti-cancerous, neuroprotective, and antioxidant properties, which are due to the presence of various terpenoids in them, whose major portion is shared by farnesene (Arslan et al., 2020; Usman and Ismaeel, 2020; Soukaina et al., 2022; Zhang et al., 2022). It also acts as a precursor to various molecules, namely vitamin E, farnesane, and squalene (Ye et al., 2022). Farnesane is a potential bio-jet fuel compound and can be used as a drop in biofuel (Richter et al., 2018b). α-farnesene also plays a major role in territorial marking and reproductive behaviour of male mice, stimulates egg laying in adult female codling moths and is also a component of sex pheromone in *Ceratitis capitata* (Morgan, 1999). The E isomer of β-farnesene is a component of several essential oils. Aphids release β-Farnesene as an alarm pheromone when they die, signalling other aphids to avoid the area (Gibson & Pickett, 1983). It is also used as an agricultural protectant for pest control (Su et al., 2015). With such multitudinous applications, the current market size of farnesene is estimated to be 1.9 million metric tons/year (Brown et al., 2016). According to Global Market Insights, the farnesene market size reached more than $315 million in 2020 and is expected to grow at over 6% compound annual growth rate in the coming years (Global Market Insights). In

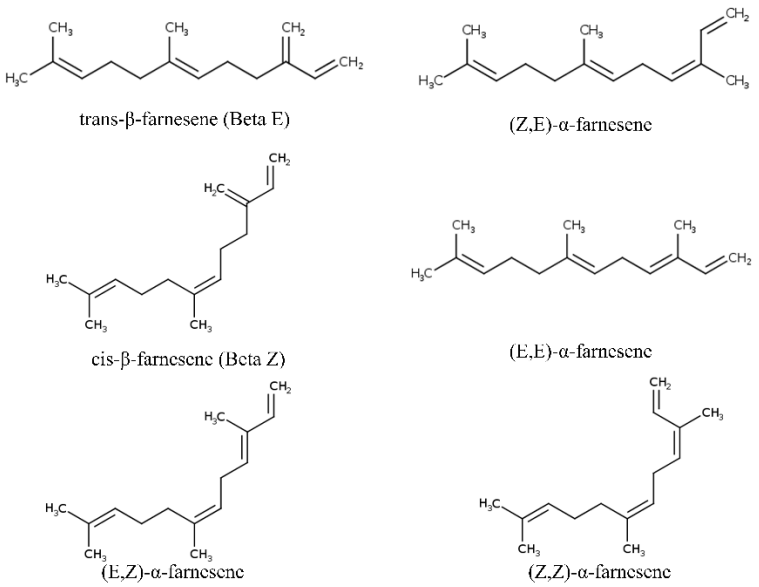

Fig. 2.1 Different isomers of farnesene

order to meet such a high market size and demand, extracting and purifying it from plants is not feasible and economical (Ma et al., 2019; Liu et al., 2019c). Chemical synthesis by trimerization of isoprene to form farnesene can meet the demand with a minimum selling price of $1.78/L but is associated with inexorable problems like high production costs and unavailability of raw materials (Bi et al., 2022). Microorganisms are propitious hosts that can be used for sustainable farnesene production. The biological sector for farnesene production is the fastest growing with a compound annual growth rate of 4.6% (Global Market Insights). Presently, USA based Amyris Biotechnologies Inc., with a manufacturing plant in Brazil, holds a significant share in worldwide farnesene production vending at a price of $1.75/L (Chandran et al., 2011; Yoo and Henning, 2017; Carvalho et al., 2022). They achieved this by utilizing a modified form of *Saccharomyces cerevisiae*, which has been genetically engineered with the farnesene synthase (*FS*) gene derived from *Artemisia annua*. In recent years other hosts, such as *Escherichia coli*, *Yarrowia lipolytica*, *Pichia pastoris*, and cyanobacteria strains, have been used for the biosynthesis of farnesene (Lee et al., 2017; Yadav et al., 2021; Ding et al., 2021; Liu et al., 2021b; Xu et al., 2023).

Plants possess both pathways to synthesize terpenoids, whereas prokaryotes (bacteria and cyanobacteria) and algae only have MEP pathway (Rautela and Kumar, 2022). Both pathways generate the same precursor molecules, IPP and DMAPP; however, MEP starts off with glyceraldehyde 3-phosphate and pyruvate, and MVA with two molecules of acetyl-CoA. Condensation of glyceraldehyde 3-phosphate and pyruvate leads to the biosynthesis of 1-deoxy-D-Xylulose-5-phosphate (DXP) with the help of the enzyme DXP synthase (dxs), which is subsequently converted to MEP. After the intermediate steps, as shown in Fig. 2.2, the 4-hydroxy-3-methylbut-2-enyldiphosphate (HMB-PP), with the aid of HMB-PP reductase enzyme, generates IPP and DMAPP, which are interconvertible with isopentenyl diphosphate isomerase (idi). On the contrary, the MVA pathway initiates with the condensation of three acetyl-CoA molecules to produce 4-hydroxy-3-methyl-glutaryl-CoA (HMG-CoA) with the aid of the enzyme acetoacetyl-CoA thiolase and HMG-CoA synthase, which is reduced to form MVA. At last, the IPP forms, which can be interconverted to DMAPP by idi (the only common enzyme in both pathways). The sequential head-to-tail condensation of IPP and DMAPP generates prenyl phosphates of varying lengths by 5 carbons. Prenyl phosphates like geranyl diphosphate (GPP), farnesyl diphosphate (FPP) and geranygeranyl diphosphate are converted to various terpenoid molecules with the help of terpene synthase enzymes. They are the key doorkeepers for the biosynthesis of terpenoids and are unique to the plant kingdom.

2.1. Biological production of farnesene through engineered microbial system

As mentioned above, terpene synthases are unique to the plant kingdom, and so is *FS*. Since the *FS* gene is usually not present in prokaryotes, engineering of the *FS* gene is foremost for the biosynthesis of farnesene from the microbial system. *FS* acts on FPP to produce farnesene (Fig. 2.2). The FS is found in apple peel with an approximate molecular weight of 66 kDa. Divalent cations such as Mg^{2+} or Mn^{2+} are required for the optimum

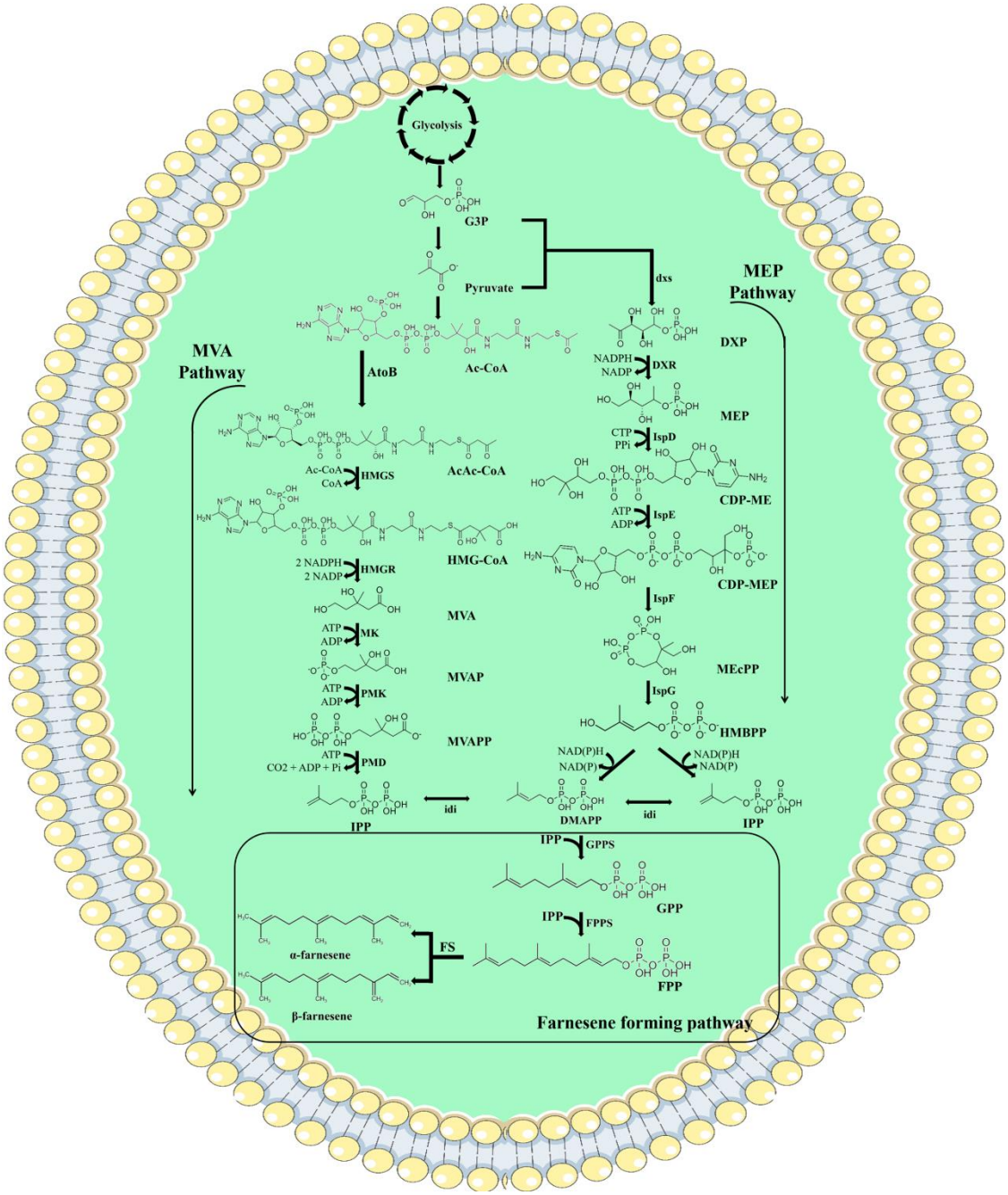

Fig. 2.2 Depiction of MVA and MEP pathways with different precursors and generating common IPP/DMAPP pool from where a common farnesene forming pathway takes place. G3P: glyceraldehyde 3-phosphate, Ac-CoA: acetyl-CoA, AcAc-CoA: acetoacetyl-CoA, HMG-CoA: 3-hydroxy-3-methylglutaryl-CoA, MVA: mevalonate, MVAP: mevalonate-5-phosphate, MVAPP: mevalonate-5-pyrophosphate, DXP: 1-deoxy-D-xylulose 5-phosphate, MEP: methylerythritol-4-phosphate, CDP-ME: 4-(cytidine 5'-diphospho)-2-C-methyl-d-erythritol, CDP-MEP: 2-phospho-4-(cytidine 5'-diphospho)-2-C-methyl-d-erythritol, MEcPP: 2-C-methyl-d-erythritol 2,4-cyclodiphosphate, HMB-PP: 4-hydroxy-3-methylbut-2-enyldiphosphate, DMAPP: dimethylallyl diphosphate, IPP: isopentenyl diphosphate, GPP: geranyl diphosphate, FPP: farnesyl diphosphate, *AtoB*: acetoacetyl-CoA thiolase, *HMGS*: HMG-CoA synthase, *HMGR*: HMG-CoA reductase, *MK*: mevalonate kinase, *PMK*: MVAP kinase, *PMD*: MVAPP decarboxylase, *DXS*: DXP synthase, *DXR*: DXP reductoisomerase, *IspD*: CDP-ME cytidylyltransferase, *IspE*: CDP-ME kinase, *IspF*: MEC synthase, *IspG*: HMBPP synthase, *IspH*: HMBPP reductase, *IDI*: isopentenyl diphosphate isomerase, *GPPS*: GPP synthase, *FPPS*: FPP synthase, *FS*: farnesene synthase.

activity of the enzyme (Pechous and Whitaker, 2004). Monovalent cation (K^+) also showed a 5-fold increase in the activity of the *FS* (Green et al., 2007). After the discovery of the *FS* gene from *Malus domestica,* several other plant sources were also identified. To engineer the *FS* gene into prokaryotes, it must be amplified from the plant cDNA. It is important to compare *FS* genes from different plant sources to discern which enzyme exhibited superior catalytic efficiency. Table 2.1 lists the catalytic properties (K_m and K_{cat}) of *FS* from various sources. Researchers have expressed *FS* from different sources in different hosts; for instance, *FS* from *M. domestica*, *A. annua*, soybean, and *Citrus jonas* in *Y. lipolytica*, *E. coli*, *Saccharomyces cerevisiae*, *Rhodobacter sphaeroides*, respectively (You et al., 2019; Liu et al., 2019c; Wang et al., 2021; Lee et al., 2022).

Farnesene synthesis by solitary expression of the *FS* gene is deficient. To further escalate the farnesene production, bottleneck gene(s) of the MEP and MVA pathway have to be engineered depending on the host organism. Different host organisms are explored for farnesene production, such as *S. cerevisiae*, *Y. lipolytica*, *E. coli*, and cyanobacteria, to name some. Fig. 2.3 represents hosts used and strains generated over the years by metabolic engineering to produce farnesene. It is evident that the choice of promoters has a vital role in controlling the expression of genes. Xu and coworkers studied the effect of 7 promoters (GAP, TEF1, GCW14, HXI11, SER1, G1, G6) on the *FS* gene expression in *P. pastoris* and found out that P_{GAP} showed the strongest activity among others giving farnesene titer of 463 mg/L (Xu et al., 2023).

Table 2.1 Michaelis Menten constant (K_m) and turnover number (K_{cat}) of farnesene synthase from various plant species.

Enzyme	Plant species	K_m (μM)	K_{cat} (s^{-1})	Uniprot ID	References
α-farnesene synthase	*Malus domestica*	10-25	0.0553	Q84LB2	Gray et al., 2011
	Actinidia deliciosa	9.5	0.440	NA	Nieuwenhuizen et al., 2009
β-farnesene synthase	*Artemisia annua*	2.1	0.0095	Q9FXY7	Picaud et al., 2005
	Zea mays (TPS10)	3.2	0.204	C7E5V7	Köllner et al., 2009
	Zea mays (TPS1)	1.0	NA	Q2NM15	Schnee et al., 2006
	Mentha piperita	0.6	NA	O48935	Crock et al., 1997

2.1.1. Farnesene production in heterotrophic organisms

Generally, two types of engineering strategies are used to express/overexpress gene(s) of interest in the host organism. First is the expression vector strategy in which the gene of interest is expressed autonomously, and second is the integration vector strategy to incorporate genes into the genome of the host. Expression vector strategy has been mostly used in engineering *E. coli* for farnesene production (Lv et al., 2019; Yao et al., 2020; You et al., 2019). Introduction and optimization of the MVA pathway in *E. coli* with co-expression of *FS* gene leads to 2.91 g/L farnesene (You et al., 2017). Yao and the group utilizing the same engineering strategy got a farnesene yield of 0.46 g/g glycerol (Yao et al., 2020). Since the FPP is the final precursor for farnesene synthesis, idi and FPP synthase (FPPS) are the two rate-limiting enzymes in its synthesis (Daudonnet et al., 1997; Wang et al., 2011; Chen et al., 2018). Increasing the number of copies of genes also proved beneficial for increasing farnesene synthesis. In *E. coli* BL21 (DE3), when *idi* and *FPPS* gene copies were increased to two with the help of an expression vector, the farnesene concentration improved by 112% (2.44 g/L) (You et al., 2019). The recombinant strain was also engineered for the ATP citrate lyase gene to increase the acetyl-CoA pool. When used in a different

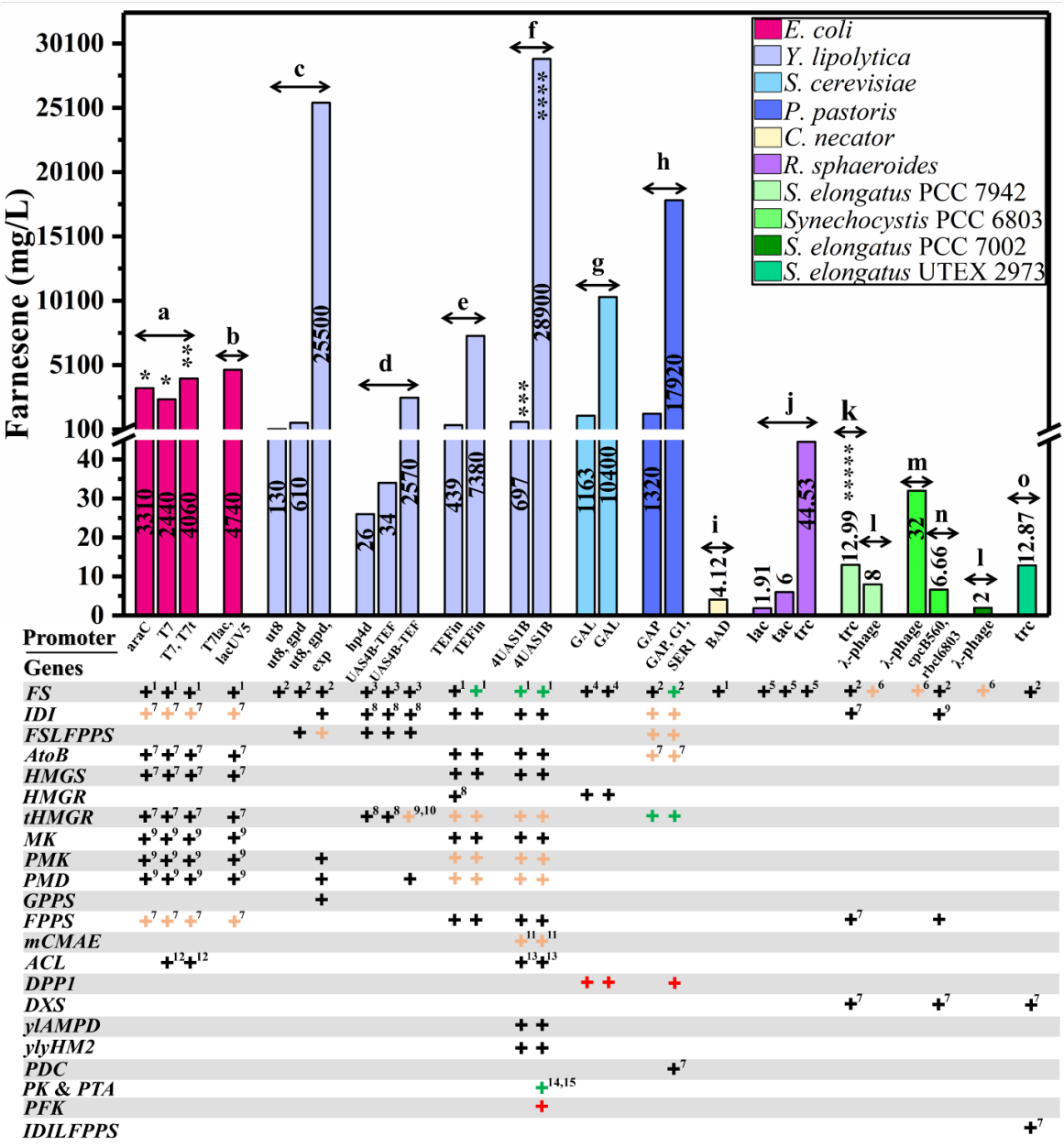

Fig. 2.3 Different host organisms used in recent years for the biosynthesis of farnesene (mg/L) by overexpressing single or multiple genes. *FS*: farnesene synthase, *IDI*: isopentenyl diphosphate isomerase, *FSLFPPS*: *FS* fused with *FPPS*, *AtoB*: acetoacetyl-CoA thiolase, *HMGS*: HMG-CoA synthase, *HMGR*: HMG-CoA reductase, *tHMGR*: truncated HMGR, *MK*: mevalonate kinase, *PMK*: MVAP kinase, *PMD*: MVAPP decarboxylase, *GPPS*: GPP synthase, *FPPS*: FPP synthase, *mCMAE*: malic enzyme, *ACL*: ATP citrate lyase, *DPP1*: diacylglycerol diphosphate phosphatase, *DXS*: DXP synthase, *ylAMPD*: adenosine monophosphate deaminase, *ylyHM2*: mitochondrial citrate carrier, *PDC*: pyruvate dehydrogenase complex, *PK*: phosphoketolase, *PTA*: phosphate acetyltransferase, *PFK*: phosphofructokinase, *IDILFPPS*: *IDI* fused with *FPPS*, The "black +" indicates the gene is expressed one time, the "orange +" indicates the gene is expressed two times, the "green +" indicates the gene is expressed three times and the "red +" indicates the deletion of a gene. Gene Source: [1]codon optimized from *Artemisia annua*, [2]codon optimized from *Malus domestica*, [3]codon optimized source not mentioned, [4]Soybean, [5]codon optimized from *Citrus junos*, [6]*Picea abies*, [7]*Escherichia coli*, [8]*Silibacter pomeroyi*, [9]*Saccharomyces cerevisiae*, [10]*Yarrowia lipolytica*, [11]*Mucor circinelloides*, [12]*Trichophyton rubrum*, [13]*Mus musculus*, [14]*Aspergillus nidulan*, [15]*Bacillus subtilis*. Unmarked + indicates that the gene source is endogenous or not mentioned. The fusion of FS and FPPS is from the respective source mentioned. * *E. coli* BL21 (DE3) strain, ** *E. coli* Transetta

(DE3) strain, *** The strain generated was also engineered with LYS2 gene (α aminoadipate reductase), **** The strain generated was also engineered with LYS2 (α-aminoadipate reductase), HIS3 (imidazoleglycerol-phosphate dehydratase), TRP1 (phosphoribosylanthranilate isomerase), URA3 (orotidine-5'-phosphate decarboxylase), and LEU2 gene (β-isopropylmalate dehydrogenase), ***** Laboratory evolved strain References – a You et al., 2019, b Ding et al., 2021, c Liu et al., 2019c, d Liu et al., 2020, e Bi et al., 2022, f Bi et al., 2023, g Wang et al., 2021, h Xu et al., 2023, i Milker and Holtmann, 2021, j Lee et al., 2022, k Pattharaprachayakul et al., 2019, l Chenebault et al., 2023, m Blanc-Garin et al., 2022, n Sun et al., 2023, o Rautela et al., 2024b.

strain of *E. coli*, Transetta (DE3), the same genetic constitution increased the farnesene production to 3.79 g/L. Further increasing the copies of *idi* and *FS* fused with *FPPS* (*FSLFPPS*) approximately doubled farnesene titer to 1.32 g/L (You et al., 2019). Similar results of improved farnesene titer were obtained in *P. pastoris* when an additional copy of *idi* and *FPPS* were introduced through an expression vector system (Liu et al., 2021c).

Integrating gene(s) in the host genome is an attractive strategy to generate stable transgenic cell factories. *Y. lipolytica* possesses an MVA pathway, and therefore the expression of mevalonate phosphate kinase, mevalonate pyrophosphate decarboxylase in conjunction with *FS*, *idi*, and *FSLFPPS* increased farnesene production from 0.13 g/L to 1.70 g/L (Liu et al., 2019c). All the genes were integrated into the chromosome by non-homologous end-joining mediated integration. Rate-limiting enzymes vary from host to host. Mevalonate kinase (*MK*) was a rate-limiting enzyme identified in *Y. lipolytica* (Liu et al., 2021b). Overexpression of *FSLFPPS* did not improve farnesene production in *Y. lipolytica*. In comparison, overexpression of *FSLFPPS* with *MK* through integration into the genome increased the farnesene titer to 2.16 g/L. Further, by expressing Vitreoscilla hemoglobin gene, the farnesene production was increased by 12.7% as the respiration of the cells improved. Integration of additional MVA pathway genes along with three copies of the *FS* gene led to a farnesene titer of 7.38 g/L in a 2 L (fed-batch) reactor (Bi et al., 2022). The same group applying a similar strategy along with the overexpression of malic enzyme, ATP-citrate lyase, adenosine monophosphate deaminase, mitochondrial citrate carrier, phosphoketolase and phosphate acetyltransferase genes and knockout of

phosphofructokinase got an increased farnesene titer of 28.9 g/L in a 2 L (fed-batch) reactor (Bi et al., 2023).

Deletion of diacylglycerol diphosphate phosphatase (*DPP1*) with the help of the CRISPR-Cas9 system in the *S. cerevisiae* (having *FS* and HMG-CoA reductase (*HMGR*) gene overexpressed) produced 1.16 g/L farnesene (Wang et al., 2021). In another study in *P. pastoris* deletion of *DPP1* with the addition of pyruvate dehydrogenase complex in the strain having three copies of *FS*, two copies of *idi*, two copies of *FSLFPPS*, two copies of acetoacetyl-CoA thiolase, and three copies of truncated *HMGR* (*tHMGR*) increased the titer from 1.32 g/L to 2.16 g/L (Xu et al., 2023). *DPP1* deletion enhances the abundance of FPP by exerting its influence on the cytosolic isoprenoid lipid phosphate phosphatase, while the addition of pyruvate dehydrogenase complex increases the acetyl-CoA pool. Similarly, deleting diacylglycerol acyltransferase in *Y. lipolytica* decreases lipid content and increases farnesene production by 45% and 33.1% (Liu et al., 2022; T. Shi et al., 2021a). MVA pathway is an energy-intensive pathway, and the inactivation of NADH-dependent dihydroxyacetone phosphate reductase increases the intracellular NADH pool in *P. pastoris*, resulting in the increased farnesene production (2.94 g/L to 3.09 g/L) (Chen et al., 2023).

Carbon source is an essential factor while using microbial cell factories. Table 2.2 summarizes the recent advances in the metabolic engineering of host organisms utilizing different substrates for farnesene production. *Y. lipolytica* can utilize waste cooking oil as a carbon source. Fatty acids in oil are converted to acetyl-CoA via β-oxidation. The strain engineered with fused FPPS with mutated *FS* (two copies), *idi* (two copies), *MK* (two copies), mevalonate phosphate kinase, mevalonate pyrophosphate decarboxylase, and GPP synthase showed a farnesene production of 1.56 g/L (Liu et al., 2022). The strain was further engineered to utilize cooking oil by overexpressing peroxisome protein, driving

farnesene titer to 2.52 g/L. The farnesene titer reached 3.34 g/L when the genes of diacylglycerol acyltransferases were deleted by CRISPR-Cas9. The final engineered strain, when grown on waste cooking oil, was able to synthesize 31.9 g/L farnesene (Liu et al., 2022). In one of the unique studies where the MVA pathway genes are engineered along with the *FS* gene in *E. coli* under the influence of isopropyl-β-D-thiogalactopyranoside (IPTG) inducible promoter, whey was used instead of IPTG to induce the gene expression (Ding et al., 2021). Replacement of IPTG with whey not only helps in the induction of promoter but also acts as a substrate for the growth of microorganisms giving dual benefits. Surprisingly the farnesene production was higher when whey was used than IPTG (2.41 g/L vs 1.46 g/L). A substantial increase in farnesene production was observed in a 7 L bioreactor with a titer of 4.74 g/L. This strategy can be taken a step ahead and used for dairy waste effluent treatment and the production of value-added products.

One of the major challenges faced by metabolically engineered microbial strains is their transition from lab-scale to large-scale production. It is evident from Table 2.2 that researchers have tried their best to upscale the production from 50 ml shake flask to up to 5 L fed-batch fermenters (Liu et al., 2020; Lv et al., 2019; Wang et al., 2021; Xu et al., 2023). It was observed that there was a several times increase in farnesene production in large-scale fermentation. For instance, engineered *Y. lipolytica* produced 0.81 g/L farnesene in a shake flask and 28.9 g/L in a 2-L fermenter (fed-batch). There was an increase in yield from 0.027 g/g glucose to 0.085 g/g glucose (Bi et al., 2023). The use of lignocellulosic hydrolysate as a carbon source slightly decreased the yield to 0.075 g/g glucose, but being a renewable and cheap glucose source, it makes the process more sustainable (Bi et al., 2022). The same engineered strain, upon metabolic pathway designing, metabolomic analysis, and fermentation test, when cultivated in a 30-L fermenter (fed-batch), reached a productivity of 3.07 g/L/day (24.6 g/L) (Liu et al., 2023a). The genetic stability of the

engineered strains also affects the industrialization of the strains. It is important for the engineered strains to bear the gene of interest without any selection for the number of generations or longer periods of time. Insertion of gene(s) into the host genome solves the stability issues (Bi et al., 2022; Wang et al., 2023). Milker and Holtmann (2021) observed that expression from a single plasmid is more stable than the two plasmids in *Cupriavidus necator*. Fermentation conditions optimization, such as medium and initial inoculum concentration optimization and C/N ratios of feeding medium with carbon source concentration optimization, can improve farnesene production and will help in achieving a level of industrialization (Bao et al., 2024).

2.1.2. Farnesene production in autotrophic organisms

The surge in the price of sugar makes it unfeasible to use them as a carbon source for manufacturing value-added goods (Cheng et al., 2019). Cyanobacteria are autotrophic photosynthetic organisms which utilize carbon dioxide and sunlight as carbon and energy sources, respectively. Therefore, they act as a sustainable host requiring carbon, phosphorus, sulfur, nitrogen, potassium, and iron sources provided by BG-11 media. Since cyanobacteria possess only the MEP pathway for terpenoid production, researchers focus on engineering and overexpressing the MEP pathway bottleneck gene(s). *Synechococcus elongatus* PCC 7942 was engineered with *FS* from *Picea abies* along with *dxs*, *idi*, and *FPPS* genes through an integration vector strategy (Lee et al., 2017). The genes were integrated at neutral sites of the genome, giving a production of 4.6 mg/L farnesene. In another study from the same lab utilizing the same host, *FS* from *M. domestica* was engineered (Pattharaprachayakul et al., 2019). The expression of the *FS* gene was modulated by ribosome binding site engineering along with overexpression of the MEP pathway (*dxs*, *idi*, *FPPS* gene). 5.66 mg/L farnesene titer was obtained in the strain with the lowest translation initiation rate. Further evolutionary engineering of the generated

strain to utilize less IPTG leads to 12.99 mg/L farnesene titer. More recently, *S. elongatus* PCC 7002 and PCC 7942 have been engineered with two copies of the *FS* gene, one copy being autonomously expressed while the other integrated at the neutral site of the genome with a titer of 2 and 8 mg/L, respectively (Chenebault et al., 2023). The highest farnesene productivity of 2.57 mg/L/day was achieved upon integration of *FS*, *dxs,* and *idi* fused with *FPPS* into the neutral sites of the genome of *S. elongatus* UTEX 2973 (Rautela et al., 2024b).

Ensuring the confinement of genetically modified strains is a matter of significant importance. The potential hazards associated with the release of modified strains and the resulting environmental risks are a cause for concern within society. In this view, strains should be generated such that they are not able to survive in ambient environmental conditions. In one such study, Lee and colleagues engineered a previous farnesene producing *S. elongatus* PCC 7942 strain (parent strain) in a manner that it is not able to survive at 100% air bubbling (ambient CO_2 condition) (Lee et al., 2021). The farnesene producing strain was overexpressed with carbonic anhydrase and bicarbonate transporter, and the β-carboxysome gene was deleted. The strain produced 5.0 mg/L farnesene, slightly higher than the parent strain (3.3 mg/L). The yield of farnesene from non-photosynthetic organisms is far better than the photosynthetic ones. The major attribution can be given to carbon partitioning, where a significant portion of the carbon is reserved for biomass synthesis and various biosynthetic pathways (Melis et al., 2023). Additional work must be done in producing farnesene from photosynthetic organisms to increase the farnesene yield by utilizing CO_2.

Table 2.2 Recent advancements in metabolic engineering of microbial cell factories for farnesene production.

Host strain	Farnesene synthase (source)	Characteristic(s) of modified strain (Vector strategy used)	Substrate utilized	Production scale (type)	Titer (g/L)	Yield	Productivity (g/L/day)	Reference
Escherichia coli	β-farnesene synthase (*Artemisia annua*)	Harbouring optimized *FS* gene. Optimized MVA pathway. (Expression vector)	Glycerol	4 L (fed-batch)	8.74	NA	1.74	You et al., 2017
			Biodiesel by-products and glycerol		2.83	NA	0.70	
		Harbouring optimized FS gene. Overexpression of *idi* and *FPPS* gene. Introduction of exogenous MVA pathway. (Expression vector)	Waste cooking oil	100 ml (shake flask)	5.29	NA	1.32	Lv et al., 2019
		Harbouring optimized *FS* gene. Optimized MVA pathway with expression of *ACL* gene. (Expression vector)	Corncob hydrolysate	5 L (fed-batch)	4.06	0.4 g/g glucose	2.03	You et al., 2019
		Harbouring optimized *FS* gene. Optimized MVA pathway. (Expression vector)	Biodiesel by-products (crude glycerol)	5 L (fed-batch)	10.31	0.46 g/g glycerol	5.15	Yao et al., 2020
Yarrowia lipolytica	β-farnesene synthase (*Artemisia annua*)	Harbouring 3 copies of optimized *FS* and *tHMGR* copies. Overexpressed MVA pathway genes. Deletion of *DGA1* and *DGA2* genes. (Integration vector)	Glucose	2 L (fed-batch)	22.8	NA	2.28	Shi et al., 2021a
		Harbouring 3 copies of optimized *FS* gene. Optimized MVA pathway. Overexpression of *idi* and *FPPS* genes. (Integration vector)	Lignocellulosic hydrolysate	2 L (fed-batch)	7.38	0.075 g/g glucose	1.23	Bi et al., 2022
		Harbouring 2 copies of MVA pathway genes and 3 copies of *FS* and *HMGR* genes with 2 copies of *mcMAE* gene. *mACL*, *ylAMPD*, *ylYHM2*, *anPK* and *bsuPTA* genes. Knockout of *ylPFK1*. (Integration vector)	Glucose	100 ml (shake flask)	0.81	0.027 g/g glucose	0.081	Bi et al., 2023
				2 L (fed-batch)	28.9	0.085 g/g glucose	2.89	

Host strain	Farnesene synthase (source)	Characteristic(s) of modified strain (Vector strategy used)	Substrate utilized	Production scale (type)	Titer (g/L)	Yield	Productivity (g/L/day)	Reference
		The strain developed by Bi et al. 2023 was modified by metabolic pathway design, fermentation test, metabolomic analysis and target mining experimental. (Integration vector)	Glucose	30 L (fed-batch)	24.6	NA	3.07	Liu et al., 2023a
			Waste cooking oil		31.9	NA	3.54	
	α-farnesene synthase (*Malus domestica*)	Harbouring two copies of optimized *FS* linked with *FPPS* gene. Overexpression of *AtoB*, *HMGR*, *HMGS*, *idi*, *MK*, *GPPS*, *PMK* and PMD genes. (Integration vector)	Glucose	1 L (fed-batch)	25.55	NA	2.12	Liu et al., 2019c
		Harbouring optimized *FS* linked with *FPPS* gene. Overexpression of *tHMG1*, *idi*, *HMGR* and *PMD* gene. (Integration vector)	Glycerol	5 L (fed-batch)	2.57	34 mg/g DCW	0.51	Liu et al., 2020
Saccharomyces cerevisiae	α-farnesene synthase (soybean)	Harbouring optimized *FS* gene. Optimization of *tHMG1* gene copies and inactivation of *DPP1* gene. (Integration vector)	Glucose	5 L (fed-batch)	10.4	NA	1.04	Wang et al., 2021
	α-farnesene synthase (*Camellia sinensis*)	Harbouring engineered *FS* gene linked with N terminal SKIK tag. Optimized MVA pathway. (Integration vector)	Glucose	50 ml (shake flask)	2.8	NA	0.70	Wang et al., 2023
				5 L (fed-batch)	28.3	NA	4.71	
Pichia pastoris	α-farnesene synthase (*Malus domestica*)	Harbouring optimized *FS* gene. Overexpression of *tHG1*, *idi*, *FPPS*. Introduced IUP pathway and pyruvate dehydrogenase encoding genes. (Expression vector)	Oleic acid/sorbitol	50 ml (shake flask)	2.56	0.88 g/g DCW	0.85	Liu et al., 2021c
		The strain developed by Liu et al. 2021c with inactivation of *GPD1* and overexpression of *cPOS5*, *ZWF1* and *SOL3* (Integration vector)	Glucose	50 ml (Shake flask)	3.09	NA	1.03	Chen et al., 2023

Host strain	Farnesene synthase (source)	Characteristic(s) of modified strain (Vector strategy used)	Substrate utilized	Production scale (type)	Titer (g/L)	Yield	Productivity (g/L/day)	Reference
		Harbouring 2 copies of optimized *FS* linked with *FPPS* gene. 4 copies of *tHMG1*, 2 copies of *idi*, 3 copies of *FS* and 1 copy of *AtoB* gene. Overexpression of *ACS* and *PDHs*, and inactivation of *DPP1* gene. (Integration vector)	Glucose	7 L (fed-batch)	17.92	0.078 g/g glucose	2.56	Xu et al., 2023
Cupriavidus necator H16 PHB^{-}4	β-farnesene synthase (*Artemisia annua*)	Harbouring optimized *FS* gene. (Expression vector)	Fructose	1 L (fed-batch)	4.12×10^{-3}	0.20 mg/g DCW	0.34×10^{-3}	Milker and Holtmann, 2021
Rhodobacter sphaeroides	cf-farnesene synthase (*Citrus junos*)	Harbouring optimized *FS* gene with RBS engineering. (Expression vector)	CO_2 and H_2	100 ml (Anaerobic)	44.0×10^{-3}	0.234 g/g CO_2	1.83×10^{-3}	Lee et al., 2022
Synechococcus elongatus PCC 7942	α-farnesene synthase (*Malus domestica*)	*dxs*, *idi*, *ispA* integrated to NSI and *AFS* integrated to NSII site. (Integration vector)	5% CO_2	100 ml (batch)	4.6×10^{-3}		0.6×10^{-3}	Lee et al., 2017
		dxs, *idi*, *ispA* integrated to NSI and *AFS* integrated to NSII. RBS engineering of *AFS* with adaptive laboratory evolution. (Integration vector)	5% CO_2	100 ml (batch)	12.99×10^{-3}	NA	1.2×10^{-3}	(Pattharaprachayakul et al., 2019)
		dxs, *idi*, *ispA* integrated to NSI and *AFS* integrated to NSII. ccm-deficient, *CA* and *bicA* overexpression. (Integration vector)	10% CO_2	100 ml (batch)	5.0×10^{-3}	NA	0.625×10^{-3}	Lee et al., 2021
	α-farnesene synthase (*Picia abies*)	*FS* gene integrated to a neutral site and cloned in expression plasmid. (Integration vector and expression vector)	NA	50 ml (shake flask)	8×10^{-3}	NA	0.38×10^{-3}	Chenebault et al., 2023
Synechocystis PCC 6803	α-farnesene synthase (*Picia abies*)	*FS* gene integrated to a neutral site and cloned in expression plasmid. (Integration vector and expression vector)	NA	50 ml (shake flask)	32×10^{-3}	NA	1.52×10^{-3}	Blanc-Garin et al., 2022

Host strain	Farnesene synthase (source)	Characteristic(s) of modified strain (Vector strategy used)	Substrate utilized	Production scale (type)	Titer (g/L)	Yield	Productivity (g/L/day)	Reference
	α-farnesene synthase (*Malus domestica*)	*FS, dxs, idi,* and *ispA* integrated at neutral site. (Integration vector)	3% CO_2	100 ml (semi-continuous)	6.66×10^{-3}	NA	2.22×10^{-3}	Sun et al., 2023
Synechococcus elongatus PCC 7002	α-farnesene synthase (*Picia abies*)	*FS* gene integrated to a neutral site and cloned in expression plasmid. (Integration vector and expression vector)	NA	50 ml (shake flask)	2×10^{-3}	NA	0.095×10^{-3}	Chenebault et al., 2023
Synechococcus elongatus UTEX 2973	α-farnesene synthase (*Malus domestica*)	*FS, dxs, idi,* and *ispA* integrated at neutral site. (Integration vector)	5% CO_2	200 ml (batch)	12.87×10^{-3}	12.48 mg/g DCW	2.57×10^{-3}	Rautela et al., 2024b

FS: farnesene synthase, *tHMG1*: truncated HMG-CoA reductase, *DPP1*: lipid phosphate phosphatase, *FPPS/ispA*: farnesyl diphosphate synthase, *idi*: isopentenyl diphosphate isomerase, *SKIK*: N-terminal serine−lysine−isoleucine−lysine, *PMD*: mevalonate-5-pyrophosphate decarboxylase, *RBS*: ribosome binding site, *AtoB*: acetoacetyl-CoA thiolase, *ACS*: acetyl-CoA synthase, *PDHs*: pyruvate dehydrogenase complex, *mcMAE*: malic enzyme from *Mucor circinelloides*, *mACL*: ATP-citrate lyase from *Mus musculus*, *ylAMPD*: adenosine monophosphate deaminase, *ylYHM2*: mitochondrial citrate carrier, *anPK*: phosphoketolase from *Aspergillus nidulans*, *bsuPTA*: phosphate acetyltransferase from *Bacillus subtilis*, *ylPFK1*: phosphofructokinase, *ACL*: ATP citrate lyase, *DGA1* and *DGA2*: diacylglycerol acyltransferase, *IUP*: isopentenol utilization pathway, *GPD1*: NADH-dependent dihydroxyacetone phosphate reductase, *cPOS5*: cytosolic NADH kinase, *ZWF1*: glucose-6-phosphate dehydrogenase, *SOL3*: 6-gluconolactonase, *CA*: carbonic anhydrase, *bicA*: bicarbonate transporter, *dxs*: DXP synthase, *DCW*: dry cell weight, *NA*: not available.

2.2. Analytical techniques for farnesene characterization

There are several analytical methods that can be employed to determine the purity, concentration, and structure of farnesene. These methods include UV-Vis spectrophotometry, high-performance liquid chromatography (HPLC), nuclear magnetic resonance (NMR), infrared spectroscopy (IR) or Fourier transformation infrared spectroscopy (FTIR), gas chromatography-flame ionization detector (GC-FID), and gas chromatography-mass spectrometry (GC-MS).

UV-Vis spectrophotometry measures the wavelengths at which farnesene molecules absorb ultraviolet (UV) or visible light. Studies have traditionally used UV absorbance measurements of crude hexane or heptane dip extracts from whole fruit to quantify farnesene (UV maximum at 232 nm) (Whitaker et al., 1997). However, this method is prone to inaccuracies due to the presence of UV-absorbing interfering substances, such as the antioxidant diphenylamine, which is commercially used to control scald (Cheng et al., 2024). Solid samples or suspensions can scatter light, leading to inaccurate readings. Additionally, the choice of solvent is crucial, as solvents with UV absorbance near the wavelengths of interest can cause interference and should be avoided (Rocha et al., 2018).

To overcome some of these limitations, HPLC is often employed. HPLC is particularly effective for analyzing farnesene due to its ability to separate compounds based on their interaction with solid and mobile phases. A reverse-phase C18 column is used due to farnesene's non-polarity. This method allows simultaneous analysis of α farnesene and conjugated trienes in apple peel extracts with dual wavelength UV detection at 232 nm and 269 nm, using methanol as the mobile phase at 0.5 mL/min. HPLC also explores the link between farnesene and trienol accumulation under varying oxygen levels, with α farnesene eluting at 3.33 minutes (Whitaker et al., 1997).

A study using acetonitrile as the mobile phase at 0.75 mL/min found hexane-extractable α-farnesene eluting at 2.8 minutes. Scald-free skin tissue had nearly three times more α-farnesene than scalding tissue at 233 nm. Due to potential overestimation or underestimation from interference by other surface components in scald-developing apples, HPLC provides a more accurate estimation of α-farnesene levels compared to spectrophotometric methods (Rupasinghe et al., 1998).

GC is often employed for a more detailed analysis to separate volatile compounds based on their boiling points and polarity, making it particularly useful for assessing the purity and composition of farnesene samples (Blumberg, 2021). Whitaker et al. (1997) analyzed HPLC-purified samples of α-farnesene through GC using a Hewlett-Packard 5890 Series II instrument equipped with a flame ionization detector (FID) and a 30 m SPB-1 column (0.20 μm film thickness) from Supelco. The analysis of the α-farnesene sample revealed a single peak with a retention time of 13.1 minutes.

The flame ionization detector is commonly used because of its consistent response, durability, high sensitivity to hydrocarbons, broad linear measurement range, and affordability (Holm, 1999). FIDs use hydrogen flames to ionize compounds based on mass flow. Despite all compounds entering the flame being burned, only hydrocarbons produce a signal that the instrument can record. The flame decomposes inorganic substances, CO_2, CO, and non-hydrocarbons that do not produce a detectable signal. As a result, the detector remains stable as contaminants are prevented from accumulating.

GC-FID enabled the direct quantification of farnesene in dodecane. FID provided a highly stable and reliable method for this quantification, showing no sensitivity drop during the direct analysis of farnesene in the dodecane overlay. Additionally, the method demonstrated reproducibility across more than 286 measurements, ensuring consistent

results. The primary drawback of FID is that it does not offer structural information, unlike MS detection (Tippmann et al., 2016a).

When structural information is needed GC-MS is the method of choice which identifies compounds based on their mass-to-charge ratio, providing high specificity and sensitivity. Direct GC-MS analysis of sesquiterpenes such as farnesene in organic overlays is effective and commonly employed, yet these overlays frequently contain other volatile, semi-volatile, or non-volatile compounds from the cultivation medium or host organism (Wang et al., 2011; Asadollahi et al., 2008). GC-MS is crucial for identifying these substances and distinguishing by-products, which is vital for metabolic engineering and strain development. Nonetheless, repeated analysis can impact the reproducibility and stability of the instrument (Tippmann et al., 2016a). Whitaker et al. (1997) conducted capillary GC-MS analyses on HPLC-purified samples of α-farnesene and conjugated trienes, utilizing Electron Impact (EI) and Chemical Ionization (CI) methods with methane and/or ammonia. These analyses were performed using a Finnigan-MAT 4510 mass spectrometer equipped with a 30 m DB-1 column (0.25 μm film thickness). The 70 eV EI spectrum matched the known profile of α-farnesene (MW = 204), as confirmed by the NIST GC-MS library, supporting the findings of Murray in 1969. Furthermore, the component showing a 232 nm absorption with a retention time of 10.7 minutes was identified as α-farnesene using both EI and methane CI GC-MS techniques.

NMR spectroscopy is another powerful tool used to characterize farnesene. Various types of farnesene, including α-farnesene, β-farnesene, and trans-β-farnesene, display unique NMR spectral characteristics that aid in their structural identification. Farnesene is typically examined using both ^{1}H and ^{13}C NMR spectroscopy, offering detailed information about the compound's molecular structure and chemical environment. The ^{1}H NMR spectrum of farnesene presents distinct signals associated with the protons in its alkene and

alkyl groups, while the ^{13}C NMR spectrum highlights the carbon environments related to its double bonds and branching (Qin et al., 2016). High-resolution spectra are obtained using instruments like the 500 MHz BRUKER (DRX-500) FT-NMR spectrometer at 25 °C. Chloroform-d ($CDCl_3$) is employed as the deuterated solvent to ensure a clean spectral background, and the spectral signal values are expressed in δ (ppm), with tetramethylsilane (TMS) as the internal standard (Sahu & Oh, 2022). ^{1}H and ^{13}C NMR spectra clearly reveal the 1,4-trans and 1,4-cis configurations of polyfarnesene's microstructure (Sahu and Bhowmick, 2019).

IR or FTIR shows substantial absorption bands that correspond to farnesene and polyfarnesene molecular vibrations and functional groups, revealing their structure and composition (Sahu and Oh, 2022). In α-farnesene, infrared properties reflect its chemical environment, including C-H stretching and bending vibrations typical of aliphatic hydrocarbons. Murray (1969) found that the =C-H stretch bands often occur between 1600-1680 cm^{-1}, whereas other peaks indicate the presence of methyl and methylene groups. According to Qin et al. (2016), (E)-β-Farnesene analogues' IR spectra exhibit substantial absorptions at 3300 cm^{-1} from N-H stretching vibrations. Strong C=C stretching vibration bands were detected at about 1600 cm^{-1}, whereas strong absorption bands around 1550 and 1370 cm^{-1} were attributed to nitro groups.

2.3. Applications of farnesene

Farnesene produced commercially from engineered microbial systems is a foundational component for creating various valuable products with multitudinous applications. Numerous variations can be brought up in the structure of farnesene resulting in utility in multiple industries. Hydrogenated farnesene finds its application in bioenergy which has a significant market value (Wang et al., 2020). β farnesene is majorly used in flavors and fragrance industry, while the polymer industry has maximum use of α farnesene

(Global Market Insights). Farnesene also aids in crop protection and can be used as an alternative to fossil-based thermoplastic elastomers. Farnesol (a farnesene derivative) is used as a flavorant to produce nicotine reward-related behaviour. Further down, we delve into the remarkable applications of farnesene and its derivatives that have enthralled researchers worldwide.

2.3.1. Biofuels

To date, four generations of biofuels have been devised. First-generation (1G) biofuels are obtained from edible, sugar-, starch-, or oil-based crops. Generally, both ethanol and biodiesel are categorized as first-generation biofuels (Lee and Lavoie, 2013). One downside of using crop residues in bulk possess a threat to the agricultural ecosystem. Continuous harvesting of crops erodes the topsoil and reduces soil fertility; hence, it is not a sustainable energy source, and consequently, second-generation (2G) biofuels were invented (Chowdhury and Loganathan, 2019; Suali and Suali, 2023). 2G biofuels can be generated from lignocellulosic crops, such as non-food parts of plants which are made to convert to biofuels. Switchgrass, stems, leaves, and husks are generally left behind after extracting food crops. 2G biofuels are sustainable, cost-effective compared to fossil fuels, and free of impurities like sulfur, nitrogen, or metals (Sarwer et al., 2022). However, 2G biofuel production is not industrially profitable, and the production procedure requires modern and costly innovations. These unavoidable shortcomings of 1G and 2G biofuels led to the emergence of third-generation (3G) biofuels. Microalgal cultivation was promoted to generate 3G biofuel feedstock as it grows rapidly and produces large amounts of lipids. Microalgae are grown on non-arable lands and consequently do not hamper the growth of feed crops. For a long time, microalgae have been cultivated to minimize the use of petroleum and, as a result, possible reduction in global warming.

Subsequently, the utilization of recombinant DNA technology emerged for the development of constructs capable of replication and exhibiting unique functionalities in both prokaryotic and eukaryotic organisms. These genetically modified organism having unique properties forms the basis of fourth-generation (4G) biofuels (Illman et al., 2000; Lü et al., 2011). Metabolic engineering of the host organism is done in such a way that traits required for biofuel production are enhanced. A plethora of research work has been done in algal metabolic engineering by genetically modifying it to produce high amounts of lipids and terpenoids, which are proven to be excellent biofuel sources (Srivastava et al., 2020). Lately, it has been reported that the hydrogenated isoprene dimers ($C_{10}H_{20}$) and derivatives of cyclobutene, cyclohexane, and cyclooctane are derived by manipulating the genome of cyanobacteria. Cyanobacterial products proved to be ideal drop-in fuel (Woodroffe and Harvey, 2022; Rana et al., 2022; Yadav et al., 2023a). Swidah and group overexpressed genes of the n-butanol pathway and deleted the acetaldehyde dehydrogenase gene for increasing n-butanol production (Swidah et al., 2018). Moreover, *E. coli* strains are extensively engineered to produce isobutanol and ethanol via the utilization of a non-fermentative pathway which can be easily adapted to favourable conditions, enabling the efficient production of these substances on a large industrial level (Srivastava et al., 2020).

Farnesene is a potential precursor molecule for biofuel generation. Farnesene, when hydrogenated to farnesane, has similar physical and chemical properties to diesel fuel (Millo et al., 2014). Appreciable combustion properties have been exhibited by farnesane, having lower heating value and cetane number. A study showed that when the engine was fuelled with a farnesane blend in diesel at full load, without any change in engine control unit calibration, brake torque levels were reported to have lower aromatic compounds and fuel density compared to diesel fuel (Millo et al., 2014). As an alternative to petroleum, drop-in biofuels are bio-hydrocarbons which is functionally identical to petroleum and can

be used in existing petroleum fuelled engines. Farnesene-based production of biofuels requires 3 main steps, namely sugar biomass pretreatment, fermentation, and thermochemical upgradation of the product (Fig. 2.4(a)). Biomass pretreatment includes a series of reactions, such as acid and alkaline treatment. Pretreatment detoxification or enzyme hydrolysis is performed prior to fermentation. After microbial fermentation, farnesene is collected by downstream processing. Finally, farnesene is hydrogenated to farnesane/synthesized iso paraffin (SIP) or hydrocracked to produce other jet fuels like *p*-cymene or limonene. Additionally, SIP can be upgraded to drop-in fuel by blending 10% of it with standard jet fuels. Oleochemical, thermochemical, biochemical, and hybrid technologies are employed to produce drop-in biofuels. Biochemical technology, which includes fermentation of sugar obtained from corn, sugarcane produces a single hydrocarbon, for instance, farnesene, alcohol, and fatty acids. This can be further upgraded to drop-in biofuels. However, the sugar used to produce biofuel contains a high oxygen level, nearly 40%. Thus, the biggest challenge of the drop in fuel is the dismissal of oxygen from the feedstock. For the dismissal of oxygen, two methods are hydrodeoxygenation and decarboxylation. The greater the oxygen content of the feedstock more it needs to be deoxygenated. This can be resolved by calculating the effective hydrogen to carbon ratio (H_{eff}/C) of the feedstock and calculated by using equation (1).

$$\frac{H_{eff}}{C} = \frac{n(H)-2n(O)}{n(C)} \quad (1)$$

Where n is the number of atoms of hydrogen (H), oxygen (O), and carbon (C).

The more the hydrogen content of the fuel better its combustion property. Since sugars and lignocellulosic materials have low H_{eff}/C, more hydrogen must be added to make the H_{eff}/C ratio close to 2, an ideal value for a finished fuel (Fig. 2.4(b)) (Karatzos et al., 2017). Hydrogen has a high auto-induction temperature; hence, its use in engines is suitable, especially when applying the blended fuel concept (Pinto et al., 2023). A study

reported that the injection of hydrogen in dual fuels such as vegetable oil and farnesane in fixed-load engines, the blend, showed reduced CO_2, CO, and particulate matter emissions. This test was carried out at 1800 rpm and fixed load engine conditions. In-cylinder pressure, fuel consumption, and pollutant emission were evaluated for these two high-reactivity fuels: farnesane and vegetable oil.

The global aviation industry has been and will expand in the coming years. The concept of bio-based jet fuels came into existence mainly because of two reasons. Firstly, with the expanding nature of this industry, there will be a surge in the employment number, which is estimated to be 90 million jobs. Secondly, jet fuel combustion increases greenhouse gas emissions, contributing around 2% of global CO_2 emissions annually (Escalante et al., 2022). The aviation industry, striving for a greener future, has pledged to reduce CO_2 emissions by 50% by 2050 compared to 2005's level. Consequently, researchers and aviation industries emphasized producing eco-friendly jet fuels. There are five technologies used to convert different compounds to bio-jet fuels, which are hydro-processed esters and fatty acid, direct fermentation to jet, ethanol to jet, gasification and fischer tropsch, and pyrolysis to jet. American Society of Testing and Materials (ASTM) has certified all these technologies except ethanol to jet and pyrolysis to jet, which are reviewed but not certified for jet biofuel production (Alves et al., 2017).

Farnesane is a paraffinic liquid, also known as 2,6,10-Trimethyl dodecane. ASTM test and specifications D7566 regarded farnesane as a drop-in fuel which is blended to 10% with Jet A1 (Escalante et al., 2022). Farnesane can be converted to jet fuels: by direct sugar to hydrocarbon. Amyris, a USA based biotech company, first utilized engineered yeast fermentation to produce farnesene and a few side products by the MVA pathway (Neuling and Kaltschmitt, 2015; Alves et al., 2017). Especially for the success of this project, yeast was metabolically engineered to consume high glucose content and transform it to

farnesene, which upon hydrogenation is converted to farnesane (Richter et al., 2018a; Goh et al., 2022).

The freezing point is a vital property of jet fuel, as the fuel should remain liquid to function even at very low temperatures. Pure farnesane and blended forms exhibit low freezing points. For instance, SIP (97 wt% of farnesane), when mixed with 10% fossil jet fuel, possesses a -90 °C freezing point. Reducing carbon chain length by hydrocracking hydrogenated terpenes

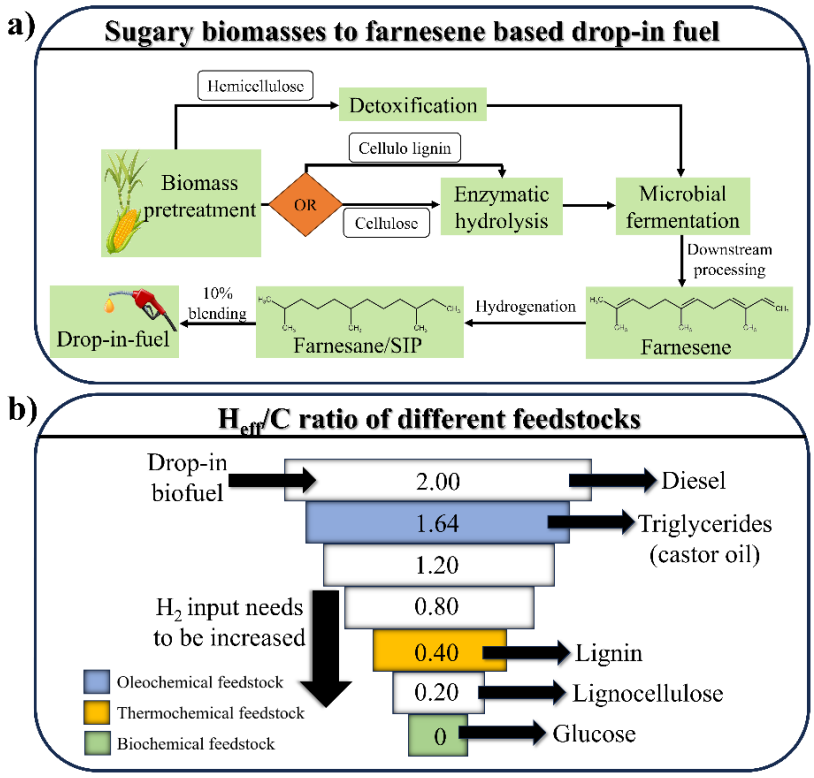

Fig. 2.4 Farnesene based drop-in biofuel production **(a)** through microbial fermentation of biomass and **(b)** analysis of H_{eff}/C ratio of various feedstocks to produce quality drop-in fuel. SIP: synthesized iso-paraffin.

is essential to lower the freezing point (Yang et al., 2019). Low-temperature fluidity is maintained by keeping the kinematic viscosity at -20 °C. The viscosity of the blended fuel must be 8 mm^2/s at -20 °C. Highly viscous aviation fuels confer pumping issues, poor atomization, and incomplete combustion (Chuck and Donnelly, 2014; Yang et al., 2019).

Although standards like ASTM D7566-18 do not specify a definitive value for derived cetane number (DCN), it is a crucial indicator of a fuel's ignition behaviour in a compression ignition engine. Higher DCN translates to a shorter ignition delay time, which ensures the complete combustion of fuel, leading to increased engine performance and cleaner emissions (Yang et al., 2019). The higher the aromatic compounds present in bio-jet fuel, the lesser the DCN value of the fuel, which implies incomplete combustion of fuel. Distillation property is essential for fuel controllability, energy integration, and product optimization. The distillation range of SIP is narrow due to the high unity of SIP fuel. The boiling point is one of the essential parameters of the distillation property.

Another indicator of fuel volatility is the flash point which aids in handling fuel parameters such as overall flammability hazards during storage and shipping. ASTM D7599-18 approves a minimum of 38 ℃ of a flash point. Contrastingly, SIP having a long carbon chain (C15) exhibits 100 ℃ as the flash point (Chuck and Donnelly, 2014; Yang et al., 2019). ASTM D7566-18 has specified a fuel density of 730-770 Kg/m^3 at 15 ℃. SIP fuel has a higher fuel density than other biofuels but is within the 765-780 Kg/m^3 range. The more the number of aromatics in fuel, the better its density. The net of combustion should be 42.8 MJ/Kg for blend fuel/conventional jet fuels except for SIP fuel (a minimum of 43.5 MJ/Kg). With an increase in aromatics net of combustion decreases. Although aromatics have an unfavourable impact on the combustion property, their presence is necessary for bio-jet fuel to obtain satisfactory properties in the fueling system. These inevitable properties of farnesane and farnesene blends are summarized in Table 2.3.

According to some reports, farnesane has been commercially used as a bio-jet fuel. Flight from Florida to Sao Paulo and from Germany was induced using 10% farnesane blended Jet A1 (de Souza et al., 2018). In addition to this, Airbus was run with farnesane from Toulouse to Hong Kong. ASTM internal standard D7566 approved 30% farnesane

blended stocks with conventional jet fuel (Michailos, 2018). Farnesane's flash point and evaporation temperature are acceptable, making it suitable for future use (Richter et al., 2018b).

Table 2.3 Comparison of fuel properties of Jet fuels and farnesene-derived blends

Properties	**20% farnesene/Jet A1[#,a]**	**50% farnesene/Jet A1[##,a]**	**SIP[b]**	**SIP (AMJ-300)[a]**	**SIP (UQJ-1)[a]**	**Amyris Farnesane[c]**	**Jet fuel[b]**
Freezing point (°C)	NA	NA	-78	97.65	40.36	-49	-47*
Initial boiling point (°C)	195	215	417	NA	NA	246.85	150*
Kinematic viscosity (at -20 °C)	8.39	5.66	14.13	3.818	7.714	NA	4.12*
Flash point (°C)	46	50	107	NA	NA	107.5	39.85*
Density at 15 °C (Kg/m^3)	790	785	495.8	768	778	770	531**
Net heat of combustion (MJ/Kg)	NA	NA	44	43.33	43.93	43	42.8*
DCN	NA	NA	NA	NA	NA	59.1	45***

[#]20% volume of farnesene blended with Jet A1, [##]50% volume of farnesene blended with Jet A1, *Jet A1 fuel, **AV-1 Brazilian jet fuel, ***JP-8 fuel. SIP: 97% farnesane, SIP (AMJ-300): 97.1% limonane with 1.6% *p*-cymene, SIP (UQJ-1): 90% farnesane with 10% limonene, DCN: derived cetane number, SIP: synthesized iso paraffin, NA: not available. References – [a]Yang et al., 2019, [b]Goh et al., 2022, [c]Feser and Gupta, 2021

2.3.2. Crop protection against aphids and other pests

Aphids are a group of 4,000 species, out of which 250 species pose serious pest problems to crops (Dixon et al., 1987). They are primarily found in temperate regions in comparison to tropical. Aphids' infestation enfeebles plants in numerous ways. They have specialized needles called stylets used as phloem sap-feeding tubes, leading to chlorosis in plants (Bhatia et al., 2011). Extracting the sap while keeping the vitality of phloem cells puts the plant at risk of other insects and pathogens. Puncturing of plant cells with stylets releases "dense" and "watery" saliva, which shields aphids from plant defence mechanisms

and prevents coagulation of plant proteins during feeding (Cherqui and Tjallingii, 2000). Some aphids and potyviruses dwell symbiotically; viruses are provided with the host for replication, and in return, virus-infected plants provide free amino acids to aphids for feeding (Guerrieri and Digilio, 2008). Virus transmission by aphids can either be persistent or non-persistent based on the time taken to inherit the virus and transmit it and the extent to which aphids remain capable of transmitting it. Persistent transmission, as the name suggests, is associated with a prolonged infection cycle which is retained lifelong by aphids and inherited by their progeny, whereas non-persistent transmission is an immediate process; aphids acquire viruses instantly through feeding infected plants but is not inheritable (Shi et al., 2021b). The major group of viruses transmitted by the aphids are potyviruses.

Owing to aphids' damage to crops and plants, there is an earnest need to control their population. The conventional and sole method for aphid population control is employing insecticides that have harmful effects on biotic and abiotic components. Fig. 2.5 shows how insecticides enter the environment. They are sprayed as aerosol and meander to the atmosphere contaminating the air. Hazardous air pollutants and volatile organic compounds in insecticides tend to volatilize and reach as high as an altitude of 4,250 m (Zhang et al., 2011). They also leach through the soil, contaminating both soil and underground water. Apart from leaching, they drift away from the source of application to the water bodies, contaminating aquatic life. Since chemicals like carbaryl are poisonous to zooplankton, reducing their number reduces the food source for aquatic animals (Metts et al., 2005). Mostly amphibians are at significant risk than birds and mammals (Hua and Relyea, 2012). Pesticide administration is inadvertently lethal to the larvae of honey bees (Wade et al., 2019). In return, this affects crop production as farmers rely upon honey bees for pollination. Repeated and improper devouring of these chemicals has led to insecticide

resistance. For instance, the whitefly *Bemisia tabaci,* which feeds over more than 600 plant species, develops resistance to insecticides and is challenging to control (Guo et al., 2020). Humans, too, have not refrained from exposure to these chemicals directly or indirectly. Forsooth humans have the highest concentration of insecticides and pesticides when they consume infected fish and crops (biomagnification) (Kesic et al., 2021).

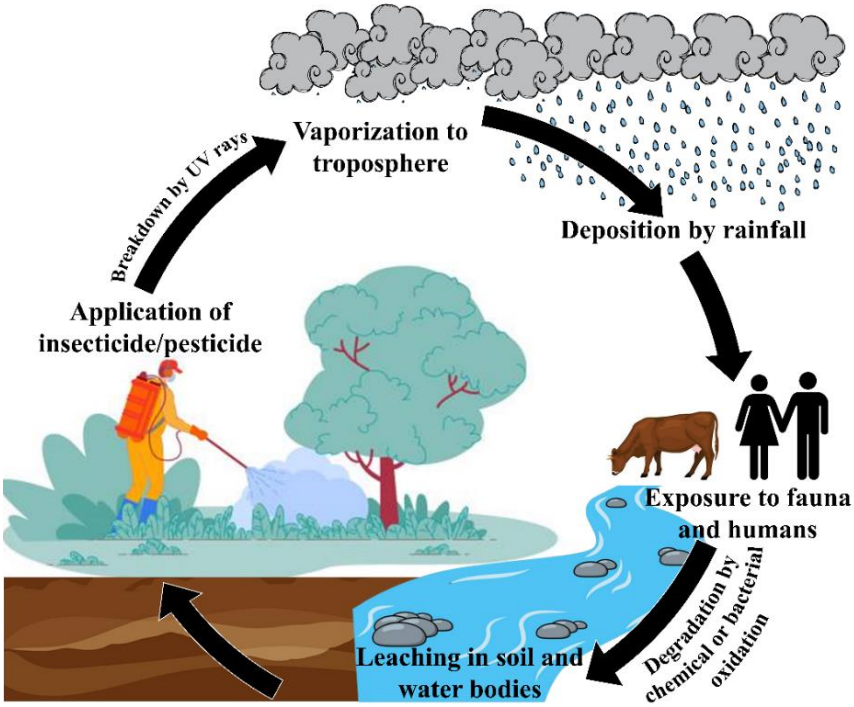

Figure 2.5 Insecticide/pesticide breakdown and movement in the environment from the site of application.

The farnesene molecule comes to the rescue to overcome the downsides of insecticides. (E)-β-farnesene (EBF), a volatile compound, acts as a semiochemical agent or alarm pheromone, which has been discerned as a possible tool for controlling aphids' population (Wang et al., 2022). Semiochemicals or alarm pheromones aid in passing signals from one organism to another, warning the recipient organism of the potential threat. Both the terms can be used interchangeably, with the fact that aphids release them as alarm pheromones alerting other aphids, and the attacked plants release them as semiochemical to attract natural enemies. Plants release these volatile compounds naturally at lower levels, and their level increases drastically when attacked by herbivores and are termed herbivore-

induced plant volatiles (HIPVs). HIPVs are a group of compounds of linalool, methyl salicylate (MeSa), decanal, methyl eugenol, (E)-caryophyllene, (E)-β-farnesene, α-bergamotene, (E)-4,8-dimethyl-1,3,7-nonatriene and (E, E) -4,8,12-trimethyl-1,3,7,11-tridecatetraene. Similar kinds of terpene molecules are released by aphids when the natural enemies detect the danger. Out of these terpene molecules, 40 aphid species release EBF (Cui et al., 2012). The researchers exploited this to use EBF as a green approach for pest control (Cui et al., 2012; Krugner et al., 2014; Lin et al., 2017; Vega et al., 2017; Zeng et al., 2017). EBF conferring resistance to plants was reported in early 1983 (Gibson and Pickett, 1983). Trichomes of *Solanum berthaultii* (wild potato) release EBF, which accords resistance from the green peach aphid. A schematic representation of the occurrence of set of reactions when aphids attack plants can be seen in Fig. 2.6(a).

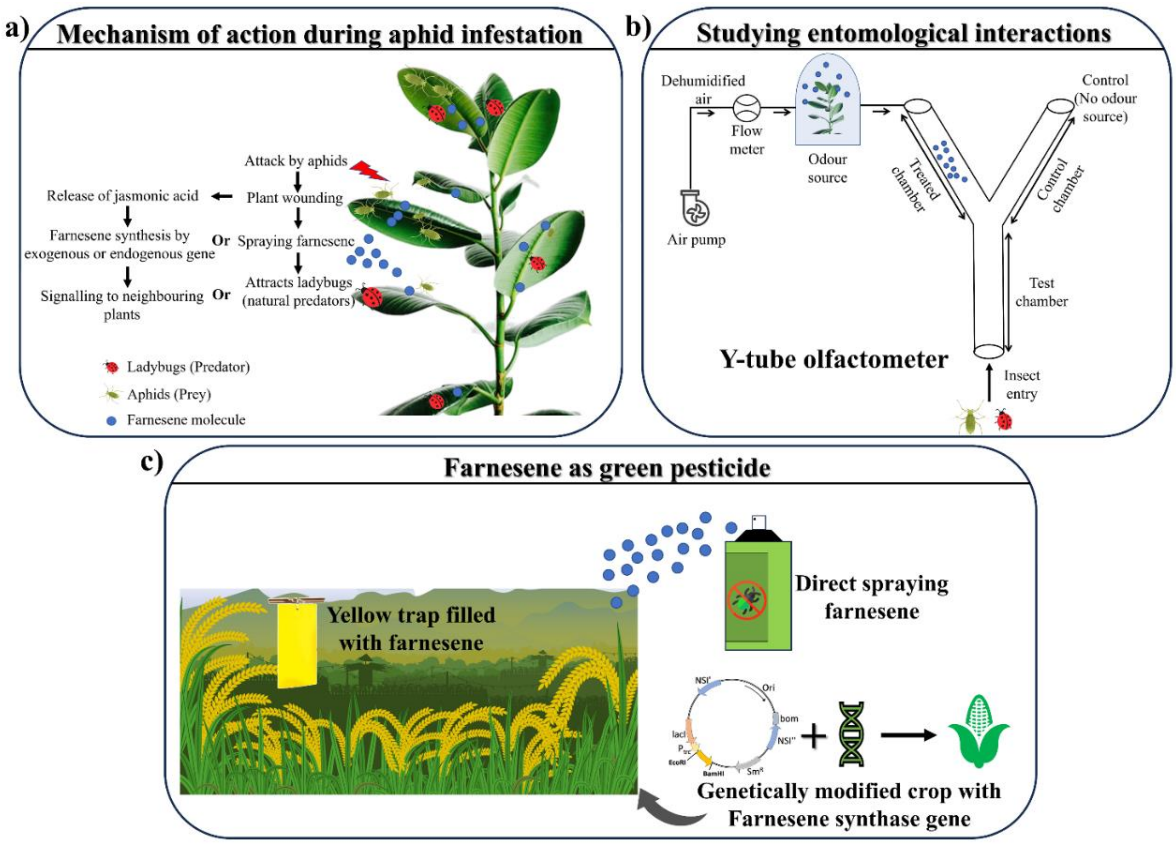

Fig. 2.6 Farnesene acting as a semiochemical agent and aiding in plant defence mechanism. **(a)** Series of reactions when aphids attack plants and farnesene is released or sprayed. **(b)** Y-tube olfactometer used in the laboratory to study entomological interactions between insects and various odours. **(c)** various ways in which farnesene can be used in crop protection.

Early studies by Cui and colleagues over the period of two years observed that EBF can attract natural predators of Chinese cabbage (Cui et al., 2012). Yellow traps (sticky traps used to record pest populations) were used for the experiment, which were filled with EBF and water as a control. EBF-released plots attracted ladybeetles, thereby reducing the aphid population. EBF filled in the yellow traps was extracted from the *Matricaria chamomilla* L., which in the lab scale allure natural enemies of aphids. In another study, a period of three years was chosen in which *Aphis craccivora* (Koch) was collected, and volatile compounds from the cornicles were extracted through the wash and adsorbent method (Kataria and Kumar, 2017). The volatile compound extracted primarily contains sesquiterpene, EBF. *A. craccivora* are difficult to manage due to their polyphagous nature. When subjected to the Y-tube olfactometer, the volatile compounds repelled *A. craccivora* and aphids of other species, *A. gossypii*, and *A. nerii*. Apart from the repulsive nature, EBF showed attraction effects to *Coccinella septempunctata*, and *Camponotus compressus*, which are bio-control agents and natural enemies of aphids, respectively. The Y-tube olfactometer is a glass Y-shaped tube through which different odorants are passed through two openings. The longer arm opening is for the insect or aphids, which are attracted or repelled by the odorants. The basic Y-tube olfactometer setup is shown in Fig. 2.6(b).

Aside from the herbivores, jasmonic acid and mechanical damage also induce HIPV formation. In *Camellia sinensis* (tea leaves), it induces majorly farnesene and ocimene production (Zeng et al., 2017). These volatile compounds generated after the damage change the metabolite profile of the neighbouring undamaged plants. Farnesene induces methyl gallate production in undamaged neighbouring plants giving the insight to use it as a pest control agent. The same was confirmed by Wang and colleagues. The group cloned tea plant *FS* into *E. coli,* which has a dual activity of converting FPP and GPP to farnesene and ocimene, respectively (Wang et al., 2019c). Later it was corroborated that wounding

activates the *FS* gene by expressing it in *Nicotiana benthamiana*. Apple orchards, when subjected to farnesene, aid in Coccinellids (ladybugs) attraction, a natural predator for aphids (Gencer et al., 2019) (Fig. 2.6(c)). Farnesene was more effective individually in comparison to the combination with linalool, benzaldehyde, and MeSa. EBF is easily oxidized in the environment and is not stable due to the presence of several double bonds. To overcome the issue, slow-release alginate beads entrapped with EBF were developed, which could release the EBF intermittently for about 15 days (Liu et al., 2021d). The mixture of EBF and MeSa in alginate beads with antioxidant tert-butylhydroquinone was most stable in controlling *Sitobion miscanthi* aphid by attracting predators. Generating a stable transgenic line of plants is another strategy in which the volatiles are constitutively synthesized, repelling aphids. One such study was done by Bruce and teammates by creating a genetically engineered wheat variety that expresses EBF synthase from peppermint (Bruce et al., 2015). The engineered wheat strain tested for *Sitobion avenae, Rhopalosiphum padi, and Metopolophium dirhodum* showed repellant activity against them.

Innumerable other pests like moths, nematodes, beetles, and mites are also potential pests to crops. Apart from physically damaging plants, some insects are natural vectors to disease-causing bacteria. The insects like Glassy-winged sharpshooter (*Homalodisca vitripennis*) and polyphagous planthopper (*Hyalesthes obsoletus*) are the vectors for bacteria *Xylella fastidiosa* and stolbur phytoplasma (Krugner et al., 2014; Riolo et al., 2017). The *Xylella fastidiosa* causes Pierce's disease, whereas stolbur phytoplasma causes yellow disease (Bois noir) in grapevine (*Vitis vinifera*). The plan of action to control *H. vitripennis* includes the release of *Gonatocerus ashmeadi,* which feeds on its eggs. It is evident from studies that *G. ashmeadi* is attracted more effectively toward a synthetic mixture of ocimene and farnesene than farnesene alone (Krugner et al., 2014). Similarly,

H. obsoletus is captivated by a mixture of five plant volatiles, including EBF, which can be used to further manage stolbur phytoplasma (Riolo et al., 2017). Cloning and expressing caryophyllene and EBF synthase genes in *V. vinifera* such that an altering blend of the volatile is released from the plant attracts *Lobesia botrana* (grapevine moth) (Salvagnin et al., 2018). This behaviour can be used in the field to control this pest.

Coffee, the most traded commodity, is greatly affected by coffee berry borer (CBB), *Hypothenemus hampei*. The estimated loss in coffee production due to CBB is around U.S. $500 million dollars (Infante, 2018). CBB is enigmatic in nature which makes the control of it difficult. Infected coffee plants release farnesene which acts as a repellent in Hawaii fields against CBB (Vega et al., 2017). In a contrasting study by Blassioli-Moraes and coworkers, farnesene does not show repellent activity but rather changes the foraging behaviour of CBB in a way by reducing attractiveness towards non-infected plants (Blassioli-Moraes et al., 2019). In a similar study, farnesene, even at different concentrations, does not show any activity against CBB (Góngora et al., 2020). Another crop of global importance is soybean, whose potential pest is soybean cyst nematode (SCN), *Heterodera glycines* (Constantino et al., 2021). The soybean *FS* gene was transformed under the cauliflower mosaic virus 35S promoter in soybean plants to generate SCN-resistant soybean (Lin et al., 2017). Upon infestation with SCN, there was a significant increase in farnesene collection in headspace compared to the non-modified strain. Further, the SCN-resistant strain showed more repellency to SCN. Moreover, the strain showed resistance to red spider mite, *ligonychus coffeae*, by attracting a natural predator. In tea plants, red spider mite infestation leads to the release of volatiles farnesene, ocimene and linalool (Rahman and Babu, 2020). These volatiles thereby aid in attracting *Neoseiulus longispinosus*, a natural enemy of red spider mites.

Understanding the interaction of aphids with volatile cues is underway. Computer simulation studies like molecular docking and dynamics reveal that there are odorant binding proteins (OBPs) that bind with the volatile ligand and pass the information to odorant receptors (ORs). Aphid's ORs being complex in nature, lack the 3D crystal structure. However, the crystal structure of OBP3 of *Megoura viciae* (MvicOBP3) and *Nasonovia ribisnigri* (NribOBP3) was determined (Northey et al., 2016). NribOBP3 solely binds to EBF, whereas MvicOBP3 binds to a mixture of volatiles (EBF, pinene, and limonene). Since the sequences of OBPs of different species are homologous, MvicOBP3 acts as an epitome for *Acyrthosiphon pisum* OBP3 (ApisOBP3). It was found that both OBPs are 97% homologous in structure (Du et al., 2018). Insights into the structure of OBPs assist researchers in discovering analogues of EBF that can efficiently and stably bind to OBPs showing superior repellent towards aphids.

EBF binds with the conjugated double bond present on the outer surface of OBP3. The binding appears to be stable as indicated by the lower root mean square deviation of 3.0 Å. Further 10 EBF analogues having substituted pyrazole and benzene rings (M1 – M10) were docked with OBP3 (Du et al., 2018). Out of these 10 analogs M1, M6, and M10 showed promising results. Inhibitory constant of M1, M6, and M10 were 1.9 μM, 2.6 μM, and 16 μM, respectively, indicating M1 has the highest binding affinity with OBP3. Besides this M1 has dual hydrogen bonds with distances 2.592 Å and 1.993 Å in comparison to M6, which only had one weak hydrogen bond. The solvent-accessible surface area of M1 was found to be 7130.04 A^2 stipulating hydrophobic interactions. In the same study, 11 analogues (N1 – N11) having triazine rings were docked. The solvent-accessible surface area of N1 suggests hydrophobic interactions similar to M1. N1 shows a similar root mean square deviation value to that of EBF. N1 also has the highest docking score of 7.42 amongst the 11 analogues proclaiming the highest binding with OBP3. In another

investigation, the commercial insect repellent (icaridin) having N-acylpiperidine was substituted with EBF to give a series of 27 acylpiperidine analogues (Li et al., 2022). These analogues showed higher insect-repellent activity than the icaridin alone. Among these 27 analogs compound 14c (E -1-(3,7- dimethylocta-2,6-dienoyl) piperidin-4-yl) methyl propionate) has the highest repellence rate of 61.3% ± 0.9, indicating that farnesene and its analogues can be used as a promising agent in crop protection.

2.3.3. Pharmacological relevance

From the days of yore plant volatile essential oils have been used as an anti-inflammatory, antifungal, and antimicrobial candidate without knowing the scientific trail of the mechanism. Plant essential oils also possess anti-cancerous, antiviral, and anti-diabetic properties. Advancements in qualitative and quantitative analytical techniques reveal that essential oils are intrinsically composed of terpenoids and phenolic compounds responsible for essential oils' properties. Flavonoids are the most abundant phenolic compounds, whereas β-phellandrene, limonene, pinene, and farnesene, are the major terpenoids found in essential oils. For instance, *Zingiber officinale* Roscoe (ginger) and its extract are well known for their medicinal properties in every household. Sesquiterpenes like zingiberene (36%), curcumene (18%), and farnesene (10%) are found in ginger's volatile oils, as are monoterpenes like cineole (1.3%), linalool (1.3%), borneol (2.2%), geranial (citral a, 1.4%), and neral (1.3%) (citral b, 0.8%) (Kiyama, 2020). Farnesene epoxide ($C_{15}H_{24}O$), a derivative of farnesene, is also a constituent of ginger extract and is an estrogen modulator acting as a chemoprotective agent. Among different species of *Artemisia*, essential oil from *Artemisia dracunculus* uniquely contains farnesene which shows anti-inflammatory properties by inhibiting human neutrophil activation and chemotaxis (Schepetkin et al., 2022). Fig. 2.7 shows the different pharmacological applications in cell lines and animal models.

Usha and her group ascertained the antioxidant activities of *Curcuma angustifolia*, *Curcuma longa*, *Hedychium* sp., and *Kaempferia rotunda* Linn (Zingiberaceae family) collected from the high altitude of Sikkim, India (Usha et al., 2017). 2,2-diphenyl-1-picryl-hydrazyl (DPPH) assay was performed to show free radical scavenging activity. The highest scavenging activity was seen with *Hedychium* sp. extract, followed by *K. rotunda* Linn. Further, the literature survey was done to find the common terpenoid molecules in the Zingiberaceae family. To name some β-phellandrene, t-linalool oxide, zingerone, farnesene, and farnesene epoxide ($C_{15}H_{24}O$, derivative of farnesene) were the selected compounds to be docked with estrogen receptor (1U3Q). β-phellandrene and farnesene epoxide showed the highest interaction with 1U3Q. Farnesene epoxide-1U3Q complex showed moderate adsorption and was favorable to cross the blood-brain barrier suggesting the anti-cancerous property of the compound. Another plant belonging to the ginger family, *Alpinia galanga* flowers essential oil, was studied for its pharmaceutical potential (Tian et al., 2022). The oil showed antibacterial activity against *Staphylococcus aureus*, *Bacillus subtilis*, *Enterococcus faecalis*, *Pseudomonas aeruginosa*, *E. coli*, and *Proteus vulgari*. In addition, it also possesses glucosidase inhibition activity, making it a promising antidiabetic agent. It was also checked for its anti-cancerous effect against K562 cells and leads to the selective apoptosis of cells with IC_{50} = 41.55 ± 2.28 μg/mL. Gas chromatography-flame ionization detector/mass spectrometry analysis of the oil reveals 57 chemical constituents (96.0%), out of which farnesene was most copious with 64.3%, followed by farnesyl acetate (3.6%) and other terpenoids. Farnesene, being the highest constituent of the oil, must have accounted for the properties of the *A. galanga* flowers' essential oil mentioned above.

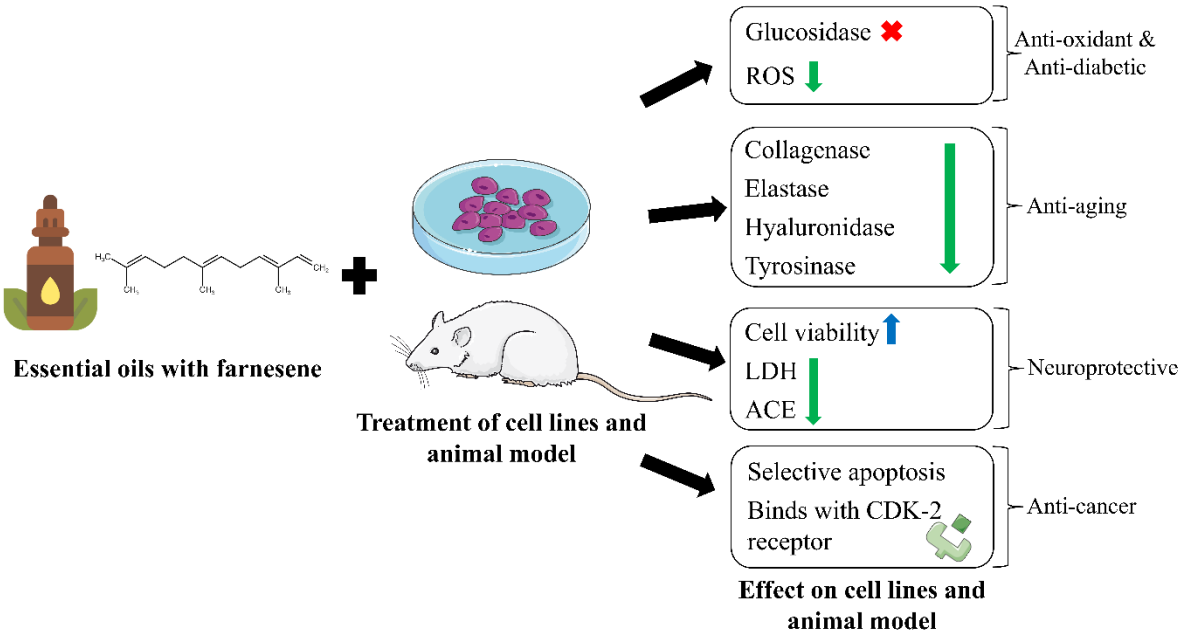

Fig. 2.7 Different pharmacological applications of farnesene on cell lines and animal models. ROS: reactive oxygen species, LDH: lactate dehydrogenase, ACE: acetylcholinesterase, CDK-2: cyclin-dependent kinase-2. The red cross denotes inhibition, the downside green arrow denotes decreased activity, and the upside blue arrow denotes increased activity.

Apart from the Zingiberaceae family plants, Lamiaceae and Asteraceae family plants are frequently used as traditional medicinal herbs worldwide to cure various illnesses. The essential oil of *Pluchea dioscoridis* (Asteraceae family) has about 25.03% farnesene, followed by ocimene and other compounds (Elgamal et al., 2021). The oil has a cytotoxic effect against MCF-7 and A-549 cancer cells with IC_{50} of 37.3 and 22.3 µM, respectively. Besides the cytotoxic effects of *P. dioscoridis* essential oil, it shows suppression towards collagenase, elastase, hyaluronidase, and tyrosinase enzymes suggesting its anti-aging properties. The study lacked the molecular docking of the constituents with the targeted enzymes which could have given more insight into the interactions of the oil constituents. In a similar study, *Phlomis aurea* Decne (Lamiaceae family) essential oil was checked for anti-cancer properties on three cancer cell lines (Human colon adenocarcinoma (HCT-116), human hepatocellular carcinoma (HepG2), and human breast adenocarcinoma (MCF-7)) and also for the antiviral activity against Herpes simplex-1 virus (Torky et al., 2021). *P. aurea* oil was able to inhibit only the HepG2 cell

line out of the three cancer cell lines with IC50 of 10.14 µg/ml. The major components of the oil were determined to be germacrene D (51.56%), pinene (22.96%), trans-β-farnesene (11.36%), and α-limonene (6.26%). Molecular docking of the constituents of the essential oil was done with cyclin dependent kinase-2 (CDK-2) receptor, which plays a pivotal role in the cell cycle. The substantial binding score was achieved by trans-β-farnesene, which was -30.64 kcal/mol, and alkyl interactions with amino acids (phenylalanine and lysine) were also seen.

The recent outbreak of novel coronavirus leading to a global pandemic which initially did not have any treatment, fascinates researchers to dock different protein targets of the virus with potential therapeutic agents. Since essential oils have antiviral properties, they are one of the therapeutic agents to be docked with the severe acute respiratory syndrome (SARS) virus. In one of this kind of study analysis of molecular interactions between 171 components of essential oils and the ligands SARS-CoV-2 main protease (SARS-CoV-2 M^{pro}), SARS-CoV-2 endoribonucleoase (SARS-CoV-2 Nsp15/NendoU), SARS-CoV-2 ADP-ribose-1"-phosphatase (SARS-CoV-2 ADRP), SARS-CoV-2 RNA-dependent RNA polymerase (SARS-CoV-2 RdRp), the binding domain of the SARS-CoV-2 spike protein (SARS-CoV-2 rS), and human angiotensin-converting enzyme was carried out (da Silva et al., 2020). Despite showing the best score, farnesene alone cannot bind to SARS covid 2 virus proteins, but the essential oil constituents can collaboratively show the antiviral properties and thus relieve symptoms.

Paclitaxel (PCX) is a chemotherapeutic agent used in the treatment of various cancers such as ovarian, lung, breast, and cervical cancers. Histopathological changes in the cochlea are brought up by PCX, inducing ototoxicity in the patients (Xuan et al., 2020). Since the number of cancer patients and the administration of chemotherapeutic drugs is increasing so is chemotherapeutic-induced ototoxicity. Previous studies suggest that the use

of antioxidants aids in the prevention and treatment of ototoxicity (Kilic et al., 2019; Sakat et al., 2019; Atalay et al., 2020). Farnesene, being an antioxidant, can be used as a treatment for ototoxicity. Dincer and group induced oxidative stress in the cochlea by giving PCX to the rats (Dincer et al., 2022). The experiment was conducted in four sound frequencies (2000, 4000, 6000, and 8000 Hz). The threshold shift in the sound frequency was measured by Distortion product otoacoustic emissions (DPOAEs) assay. Threshold DPOAEs were less in PCX given rats in comparison to the control group (where no PCX and farnesene were given) after 22 days. When farnesene and PCX were given to the ototoxic rats there was a significant increase in threshold DPOAEs. This was since farnesene protected cochlea from oxidative stress induced by PCX. Aside from the properties mentioned above farnesene exhibits neuroprotective properties. In two independent studies from the same laboratory, protection against neurotoxicity by farnesene was demonstrated. In the first study, hydrogen peroxide (H_2O_2) was used to induce oxidative stress in neuronal cells leading to neurotoxicity (Turkez et al., 2014). Further, the farnesene isomers and their mixture were tested for protection against H_2O_2-induced cytotoxicity. H_2O_2 generates reactive oxygen species and inhibits cortical neuronal cell growth with an increase in lactate dehydrogenase (LDH) levels. H_2O_2 treated cortical neuronal cells, when treated with farnesene, increased cell viability and decreased LDH activity, thus preventing neurodegeneration. The maximum neuroprotective properties were observed by β-farnesene followed by a mixture of farnesene isomers and α-farnesene. The possible mechanism of action of neuroprotective properties was suggested to be through antioxidant and antigenotoxic properties. In the second study from the same group Alzheimer's model was created by differentiating the Human neuroblastoma cell line (SHSY-5Y) into neuron-like cells by the application of retinoic acid (Arslan et al., 2020). Further, the β-amyloid was added to the transformed cells to mimic Alzheimer's cytotoxicity. The transformed

Table 2.4 Farnesene content in different essential oils and properties possessed by them.

Essential oil source	Farnesene content (%)	Properties	References
Peperomia pellucida (L.) Kunth	22.20	Therapeutic	Usman and Ismaeel, 2020
Tanacetum cinerariifolium Schultz Bip. (Asteraceae)	71.00	Plant defence mechanism	Li et al., 2021
Anthriscus nemorosa	4.00	Antitrypanosomal	Baldassarri et al., 2021
Tinomiscium petiolare	4.54– 4.65	Antimicrobial	Thinh et al., 2021
Andryala pinnatifida subsp. mogadorensis	14.92	Antioxidant and antibacterial	Soukaina et al., 2022
Polygonum aviculare	19.46	Semiochemical agent	Demirpolat, 2022
P. persicaria	25.00		
P. lapathifolium	6.20		
P. arenarium	13.86		
P. bellardii	12.26		
P. arenastrum	20.75		
P. cognatum	9.49		
Gardenia jasminoides	10.24	Medicinal and Industrial value	Zhang et al., 2022
G. jasminoides f. longicarpa	32.45		
Rhododendron anwheiense Flowers	23.80	Antioxidant, anti-melanogenesis	Chen et al., 2022
Teucrium polium L.	11.66	Repellent against mosquito	Tahghighi et al., 2022
Lagoecia cuminoides	16.40	NA	Bahmanzadagan et al., 2022
Matricaria chamomilla L.	24.30	Phytopesticidal efficiency	Al-Ghanim et al., 2023
Phlomis olivieri Benth. shoots	5.10–18.40	NA	Salehi and Kalvandi, 2023

NA: not available

cells, after treatment with farnesene, showed promising results by decreasing cytotoxicity and protecting chromosome integrity. Besides the cell viability and LDH assay, an acetylcholinesterase (ACE) assay was conducted, showing farnesene treatment significantly decreased ACE activity in the culture (in contrast to the β-amyloid

applications where ACE activity was high). Farnesene content in different plant essential oils is summarized in Table 2.4. Though farnesene shows encouraging results as a pharmacological agent, further research is required to completely discern the pharmacological relevance of farnesene and to ascertain its safety and efficacy in human beings.

2.3.4. Thermoplastic elastomers

Thermoplastic elastomers (TPEs) refer to a group of polymers that are flexible, possessing both thermoplastic and elastomeric properties. They are extensively used in fabricating products that require rubbery properties, namely seals and gaskets, and can be over-moulded at high temperatures. TPEs are biphasic in nature, which explains their soft rubbery and hard crystalline domain (Fig. 2.8) (Aiswarya et al., 2022). The two phases are bonded to each other by block, graft, and star-branched polymerization. Various types of TPEs exist, classified according to the specific polymerization method used to bind the two distinct phases together. These are styrene-based TPEs, combinations of hard polymer segment and elastomer, grafted copolymers, number of blocks of different copolymers and skin-core type of morphologies (Zanchin and Leone, 2021). Thermoplastic styrenic elastomers have outstanding flexibility and elasticity and are the most rubber-like among the other TPEs. Anionic polymerization is employed for Styrenic TPEs. Anionic and cationic polymerization is a type of ionic polymerization that depends on the type of initiators used. Extreme care is required during polymerisation on account of the very high reactivity of these ionic groups towards any impurities present in the system (Luk et al., 2021).

Polystyrene can be used as the hard component, and different products can be synthesized by varying the soft components, for instance, SBS (S: styrene, B: butadiene), SIS (I: isoprene), SEBS (E: ethylene, B: butylene) and SEPS (P: propylene). SBS and SIS

are generally used in footwear, adhesives, and asphalt enhancers. SEBS and SEPS are mainly used in soft moulded materials, in resin (polyolefin and polystyrene) enhancers, and in adhesives because of their excellent thermal and weather resistances (Maji and Naskar, 2022). Polymers derived from fossil fuels, including butadiene and isoprene, have been used for a long time (Wahlen and Frey, 2021). Both butadiene and isoprene have low glass transition temperatures (T_g), which can be increased by introducing a hard component like styrene or acrylonitrile, making the polymer soft and flexible like rubber. Two examples of rubber are styrene butadiene rubber (SBR) and nitrile butadiene rubber (NBR), which are produced by copolymerizing butadiene with styrene and acrylonitrile, respectively (Bertin et al., 1995; Kopal et al., 2018).

Fossil fuel resources exploitation to generate thermoplastic materials and rubbers was overwhelmingly affecting the environment, reflected as global warming, smog, and emission of poisonous gases. Sustainable and harmless alternatives are being sought, which are of natural origin and have a lower carbon footprint. Reports considered farnesene, myrcene, and ocimene as potential bio-based sources for polymerization holding similar properties to petroleum-derived polymers such as 1,3-butadiene and isoprene. Amongst the diene class of monomers, β-farnesene is one of the most investigated polymers with small molecular weight and distinctive structure-property relationships (Yoo and Henning, 2017). Polymerization of trans-β-farnesene and myrcene produces "bottlebrush-like structures" with critical molecular weight Mc = 50 Kg/mol, below which it behaves like bottlebrush-shaped polymer and holds rouse-like melt dynamics. When the molecular weight of the polymer exceeds a critical point, it acts as a tangled network of polymer melt. Bottlebrush exhibits reduced melt and solution viscosity, making poly-farnesene an alternative to linear polyisoprene for enhancing styrene-based TPEs processing. Moreover, it can be consumed as lubricants, hydraulics, fluids, cosmetics, and adhesives (Luk et al., 2021; Wahlen and

Frey, 2021; Luk and Maric, 2021). Polyfarnesene has low melt viscosity because of its high entanglement molecular weight. Low viscosity ushers the mixing and blending of various components in TPEs formulations and improves melt flow properties which in turn enables the material to flow easily, ensuring better mould filling and reducing the likelihood of defects such as voids (Yang et al., 2023a). Figure 7 shows the chemical structures of farnesene-based polymers and their properties.

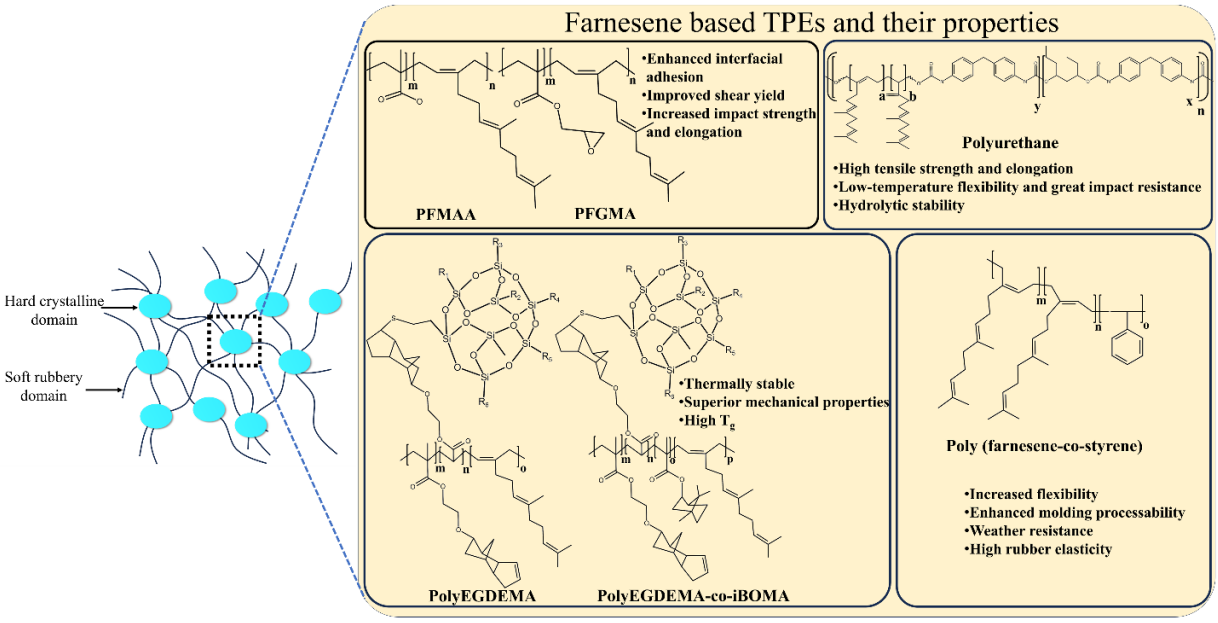

Fig. 2.8 Illustration of the hard and soft domains in thermoplastic elastomers (TPEs) and chemical structures of farnesene based TPEs with their properties. PFMAA: poly (farnesene-co-methacrylic acid), PFGMA: poly (farnesene-co-glycidyl methacrylate), EGDEMA: ethylene glycol dicyclopentenyl ether methacrylate, iBOMA: isobronyl methacrylate.

Aromatic vinyl compounds like styrene, α-methylene and 2-methyl styrene reacts with farnesene in the presence of a solvent and Lewis base to obtain block copolymer. Lewis base (dibutyl ether, diethyl ether and tetrahydrofuran) is used to control the microstructure of each constitutional unit derived from farnesene (Sasaki et al., 2014). Newmark and Majumdar (1988) polymerized biobased dienes like myrcene and farnesene by living anionic polymerization using sec-butyl lithium (sec-BuLi) in cyclohexane. In another study, diene/styrene monomers in cyclohexane resulted in tapered diblock in each step of polymerization (Wahlen et al., 2020). Soft polymyrcene can be sandwiched between the end blocks of hard poly (L-lactide). These end blocks were then reacted with ethylene

oxide, which resulted in hydroxy-terminated end groups, which were then used as micro initiators for ring-opening polymerization of L-lactide. It is reported that statistical anionic copolymerization of myrcene with common comonomers like isoprene and styrene using sec-BuLi as an initiator generated polymers with high molecular weight and low dispersity (Zhou et al., 2016; Grune et al., 2019). Zhang et al. (2019b) synthesized partially sustainable rubber by introducing β-farnesene in a polymerized butadiene-styrene solution, copolymerized by anionic polymerization. Styrene in the co-polymer improves the rolling resistance properties. The incorporation of farnesene was found to increase the tensile strength of rubber or elastomer (Banda-Villanueva et al., 2022). Polyfarnesene was synthesized in heptane by anionic polymerization using n-butyl lithium as an initiator exhibiting T_g (-73 °C) (Iacob et al., 2018). Poly (trans-β-farnesene) diols and monols are produced with hydroxyl-termination of both chain ends using a bifunctional initiator (Yoo and Henning, 2017). Thus, bio-based dienes like myrcene and farnesene were successfully polymerized using anionic polymerization. Reversible deactivation radical polymerization (RDRP) of bio-based dienes differs from ionic polymerization, as only dissolved oxygen needs to be removed for RDRP reactions (Szwarc, 1956; Shipp, 2006). Among the various methods of RDRP, nitroxide-mediated polymerization (NMP), atom-transfer radical polymerization (ATRP) and reversible addition-fragmentation chain transfer (RAFT) are well-established. However, ATRP and RAFT polymerization of farnesene have not been investigated so far (Luk et al., 2021).

NMP was employed to synthesize polymers of myrcene and farnesene with styrene using succinimidyl-modified bloc-builder (SG1-based NHS-BB) initiator to make a block and random copolymers. Farnesene, when copolymerized with methacrylate and isobronyl methacrylates (iBOMA) using NHS-BB initiator gives T_g = -70 °C which is close to petroleum-based polymers, (poly) butadiene, and (poly) isoprene having T_g = -100 °C (Luk

and Maric, 2019; Luk and Maric, 2021). Similarly, when copolymerized with iBOMA, myrcene terpene-based diene exhibits high thermal stability and elasticity with T_g = -70 °C. Dispolreg 007 (D7) initiators show better linear polymerization kinetics and keep going with more active chain ends as compared to NHS-BBs (Bertin et al., 1995). Diene triblock copolymers such as tertiary butyl alcohol, iBOMA and dimethyl acrylamide, when incorporated collectively, proved to improve the mechanical strength of the polymer as compared to the styrene analogues (Luk et al., 2021). One shortcoming of NMP is its ineptitude to homopolymerize methacrylates while maintaining active chain ends due to the steric stability of the methacrylate giving radical and steric hindrance from the bulky SG1-based nitroxide. Table 2.5 summarizes recently developed farnesene-based polymers.

Amyris Inc. filed a patent reporting the use of pressure-sensitive adhesives for the polymerization of farnesene. The patent noted that co-polymerization with sulfur dioxide showed good adherence to surfaces such as wood, aluminium and copper (Mcphee, 2010). Fina Technology Inc. holds many patents using polyfarnesene in various applications. One includes the importance of Fridel-Craft catalysts to synthesize polyfarnesene having low molecular weight as resins blended with elastomers. Another patent details the anionic polymerization of farnesene with at least one hydroxyl-terminated chain end for changes such as hydrogenation or acrylation (Yoo et al., 2015). A liquid optically cleared polymer was produced which can be used in laminated screen assemblies of electronic devices. Trans-β-farnesene performs diel-alder reactions with various dienophiles such as methyl acrylate, pentafluorophenyl acrylate, maleic anhydride, and dimethylacetylene dicarboxylate, resulting in a polymer with thermal stability at high temperatures, 250 °C (Luk et al., 2021).

As discussed earlier, there are many advantages of farnesene as a polymer. Properties such as tensile strength and sustainability make it reliable for long-term use and

reduce the use of fossil fuels for polymer synthesis (Banda-Villanueva et al., 2022). Moreover, farnesene or myrcene-based polymers show excellent mechanical strength and chemical resistance for instance, Halloran et al. (2022) first explored trans-β-farnesene and other farnesene blends (Poly (farnesene-co-glycidyl methacrylate) and Poly (farnesene-co-methacrylic acid)) as rubber toughening agents, consisting properties to enhance the impact strength of poly (lactide). However, the use of myrcene copolymers has been reported to upgrade the mechanical properties of polyurethane and poly(lactide) (Zhang et al., 2019b). Even though farnesene is a promising polymer, scaling up and maintaining quality holds challenges. Hopefully farnesene's commercialization as a thermoplastic elastomer may be accelerated by ongoing advances in biotechnology and process engineering.

2.4. Miscellaneous applications

Apart from the applications discussed, farnesene is used as a flavorant and odorant. It is also used in the cosmetic industry. The characteristic smell of various plant essential oils is due to the presence of various terpenoids, out of which one can be farnesene. *Citrus hallabong* peel oil has a characteristic odour due to the presence of farnesene (Choi, 2003). Farnesene has a relative flavor activity of 14.1 in hallabong peel oil and is therefore regarded as a character impact odorant. Fresh jasmine flower tea is famous in many parts of the world due to its relaxing and antioxidant properties. α-farnesene was found to be the most profuse volatile emitted by jasmine flowers (Yu et al., 2017). The stage of the flower used for infusion is essential to obtain the maximum benefits of the tea. The farnesene content was highest (53.86 mg/kg fresh weight) at the flower opening stage and reduced afterwards. After the excision of the flower, it remained at 30.66 mg/kg fresh weight up to 16 h. Therefore, flowers at the opening stage and fully bloomed flowers up to 16 h can be used to make jasmine tea.

Table 2.5 List of recently developed farnesene-based thermoplastic elastomers.

Type of polymerisation	Reactants	Initiator/catalyst	Solvent	Reaction temperature (°C)	Product	T_g (°C)	References
Statistical anionic copolymerisation	β-farnesene + Styrene	Sec-BuLi	Cyclohexane	23	Poly(farnesene-co-styrene)	-64.15	Wahlen et al., 2020
Anionic polymerisation	Polyfarnesene diol + EHD	NA	MDI	60 → 80 → RT	Polyurethane	-66	Zhang et al., 2019b
	Trans-β-farnesene + 3,4 vinyl compounds	n-butyl lithium	Heptane	40	Polyfarnesene	-73	Iacob et al., 2018
Free radical polymerisation	Trans-β-farnesene + glycidyl methacrylate + poly lactide	NA	Xylene	50 → 175	20-PFGMA	-68	Halloran et al., 2022
	Trans-β-farnesene + methacrylic acid + Poly lactide	NA	Xylene	50 → 175	20-PFMAA	-68.6	
Coordination polymerisation	Polyfarnesene + cellulose nanocrystals	NdV_3, DIBAH, Me_2SiCl_2	Cyclohexane	70	Fully biobased elastomeric nanocomposite	-76	Magaña et al., 2021
Reversible deactivation radical polymerisation	β-Farnesene + EGDEMA	D7	Toluene	90	Poly(EGDEMA-β-farnesene)	28	Luk and Maric, 2021
	β-Farnesene + EGDEMA + iBOMA	D7	Toluene	90	Poly(EGDEMA-Co-iBOMA-β-farnesene)	190	

DIBAH: diisobutyl aluminum hydride, D7: dispolreg 007, EGDEMA: ethylene glycol dicyclopentenyl ether methacrylate, EHD: 2-Ethyl-1,3-hexanediol, H_2Pd/C: hydrogen, palladium and carbon, iBOMA- isobronyl methacrylate, MDI: liquefied diphenylmethane diisocyanate, Me_2SiCl_2: dimethyl dichlorosilane, NA: not available, NdV_3: neodymium versatate, PFGMA: poly farnesene-co-glycidyl methacrylate, PFMAA: poly farnesene-methacrylic acid, RT: room temperature, Sec-BuLi: secondary butyl lithium, T_g: glass transition temperature.

According to the World Health Organization, smoking is the most common customary form of tobacco consumption. It kills around 8 million people worldwide, including 1.2 million deaths from secondary smoking. Nicotine, the main substance responsible for addiction to tobacco, triggers the release of dopamine neurotransmitters by activating nicotine acetylcholine receptors (nAChRs) (Engle et al., 2013). This gives a person a pleasurable feeling, termed nicotine reward-related behaviour. Due to active campaigning and health concerns, there was a decline in the consumption of combustible cigarettes, which shifted towards e-cigarettes or electronic nicotine delivery systems (ENDS). The ENDS became rapidly popular among teenagers due to the presence of innumerable flavor options. Menthol is the most preferred flavor while smoking as it enhances nicotine reward-related behaviour and upregulates nAChRs and is therefore commonly used in ENDS flavoring. Since menthol has a lower cessation rate, other alternatives to it are being searched (Miech et al., 2023).

Green apple and other fruity flavors are being explored to be used in ENDS. Farnesol and farnesene are the two chemical flavorant of green apple and are studied by researchers for producing reward-related behaviour. Avelar and group discovered farnesol produced reward-related behaviour in male mice, enhancing locomotor activity (Avelar et al., 2019). Farnesol administration showed upregulation of nAChRs and ventral tegmental area dopamine neuron firing. A year later, Cooper et al. (2020) studied another green apple flavorant, farnesene and discovered its reward-related behaviour in both male and female mice. Though farnesene administration doesn't upregulate nAChRs and ventral tegmental area dopamine neurons significantly, extended use of it as a therapeutic method modifies the composition of nAChRs, making them highly responsive. Similarly, essential oil from *Chrysanthemum morifolium* consists of farnesene as a major constituent (14.58 μg/g)

(Chun-Ping et al., 2015). 1% of the essential oil was found optimal to be used as cigarette flavor. It is discerned to reduce bitterness and increase sweetness while smoking.

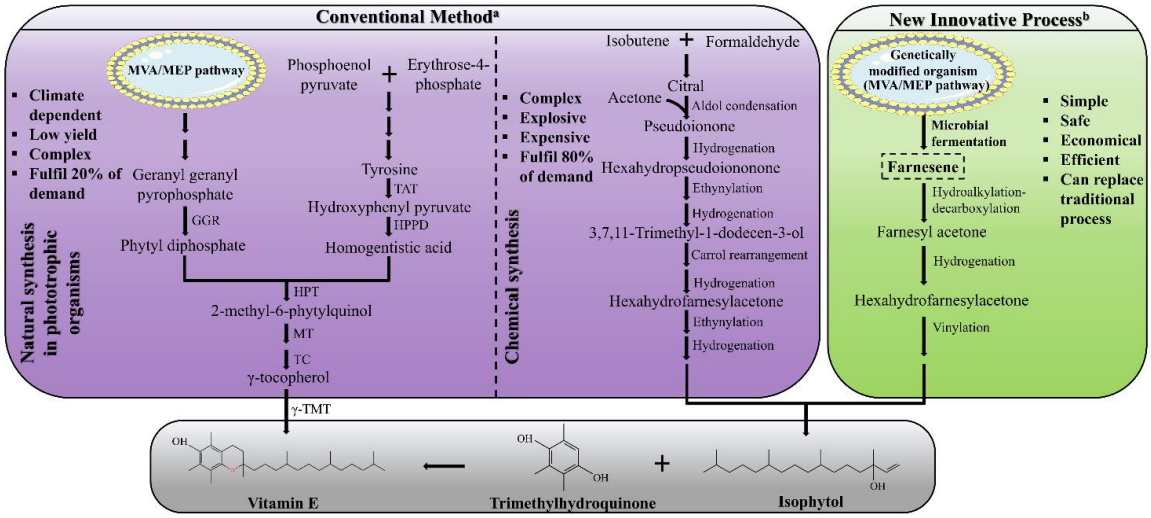

Fig. 2.9 Vitamin E synthesis from conventional and new innovative processes. *GGR*: geranyl geranyl reductase, *TAT*: tyrosine aminotransferase, *HPPD*: 4-hydroxyphenyl pyruvate dioxygenase, *HPT*: homogentisate phytyltransferase, *MT*: 2-methyl-6-phytylbenzoquinol methyltransferase, *TC*: tocopherol cyclase, *γ-TMT*: tocopherol methyltransferase. For a detailed MVA/MEP pathway, refer to Figure 1. References – [a]Ogbonna, 2009, [b]Ye et al., 2022.

Melanin is produced by the skin as a defence against UV exposure. This leads to pigmentation or hyperpigmentation, which can be treated by kojic acid, arbutin and other chemicals, having some side effects. Plants' natural extracts are well known to possess anti-melanogenesis activity and are on the safer side. Citrus fruit essential oil contains farnesene and other terpenoids, which are responsible for the anti-melanogenesis activity (Yang et al., 2023b). Farnesene was then individually tested and was found to be a potent skin-whitening agent similar to kojic acid. Vitamin E, α-tocopherol, is known for its antioxidant, anti-inflammatory, and anti-cancerous properties and is used in cosmetics, medicines, feedstock, and other industries. Extraction of Vitamin E from natural sources only fulfils 20% demand. The chemical synthesis of Vitamin E is achieved from the condensation of trimethylhydroquione and isophytol (Fig. 2.9). Isophytol formation is a complex process and is explosive in nature, and begins with the condensation of citral and acetone. In view of this, farnesene is seen as a safer alternative that can be easily converted to isophytol and,

hence, α-tocopherol. In a recent study, *S. cerevisiae* was modified to produce fermented farnesene (55.4 g/L). The farnesene was further converted to isophytol in three steps with a yield of 92% (Ye et al., 2022). It is anticipated that this new process can make the conventional method obsolete.

2.5. Techno-economic analysis and life cycle assessment of farnesene production

In an era where sustainability concerns and economic viability are at the forefront of decision-making processes, the integration of techno-economic analysis (TEA) and life cycle analysis (LCA) has emerged as a powerful approach for evaluating the feasibility and environmental impact of various technologies, products, and processes. TEA and LCA offer complementary perspectives, combining economic assessment with environmental evaluation to provide comprehensive insights into the sustainability and efficiency of systems. TEA is a systematic methodology utilized to assess the economic viability of a technology or process. Whereas, LCA is a holistic approach used to evaluate the environmental impacts associated with a product, process, or service throughout its entire life cycle—from resource extraction and manufacturing to use and disposal (Koch et al., 2023).

The integration of TEA and LCA offers several advantages, allowing for a more comprehensive assessment of the sustainability and efficiency of technologies, products, and processes. By combining economic analysis with environmental evaluation, decision-makers can identify synergies and trade-offs between financial performance and environmental impact, facilitating the development of strategies that reconcile economic prosperity with environmental stewardship. Additionally, TEA-LCA integration enables the identification of cost-effective opportunities for reducing environmental footprints and enhancing resource efficiency, thereby promoting sustainable development and long-term resilience (Mahmud et al., 2021; Wunderlich et al., 2021).

TEA and LCA studies involve 6 major steps, namely, inventory analysis, impact assessment, TEA modelling, LCA modelling, sensitivity analysis, and decision-making (Gangwar et al., 2024). Inventory analysis involves gathering data on the costs of the resources consumed and emissions generated at each stage of production. This includes the cost of raw materials used, equipment and their installation, salaries, overhead expenses, and land. Further, the environmental impacts defined in inventory analysis are categorized into global warming potential, eutrophication, and human toxicity. Using software like Aspen Plus, SuperPro Designer, and BioSTEAM, the TEA model is constructed to evaluate the economic feasibility of the production plant (Canizales et al., 2020; Cortes-Peña et al., 2020; Nikoo and Mahinpey, 2008). TEA modelling aids in assessing capital and operating costs, minimum selling price, revenue streams, and internal rate of return. Similarly, LCA modelling is done using SimaPro, OpenLCA, GaBi, and CCaLC2 (Adsal et al., 2020; Herrmann and Moltesen, 2015; Pamu et al., 2022). LCA modelling quantifies environmental impacts and identifies opportunities for environmental improvement. To assess the robustness of the TEA and LCA modelling sensitivity analysis is done by varying key parameters in the production process. Finally, a decision is made whether the process is economic and environment friendly. This involves optimizing production processes and identifying opportunities for cost reduction or environmental improvement.

The commercial production of farnesene is dominated by Amyris Inc., USA, which utilizes yeast and sugarcane as a feedstock for farnesene production. The TEA and LCA studies of conceptual farnesene production plants conducted until now utilize sugarcane as a feedstock (Michailos, 2018; Moreira et al., 2014; Santos et al., 2018). In previous studies, jet fuel (farnesane) production was shown. One of the major drawbacks of using sugarcane as biomass is pretreatment which involves dilute acid, dilute acid combined with alkaline treatment, steam explosion, steam explosion combined with alkaline treatment, organosolv,

alkaline wet oxidation, liquid hot water and liquid hot water combined with alkaline treatment (Santos et al., 2018). This not only adds up to the production cost but also is not environmentally friendly. After the biomass pretreatment, several processes like ethanol to jet, direct fermentation, fast pyrolysis and gasification Fischer- Tropsch are used to generate jet fuel. Fast pyrolysis was the most economical method, generating the lowest minimum jet selling price. The TEA of fermentation of sugars to farnesane shows the minimum jet fuel selling price to be $2.78/L (Michailos, 2018). The LCA study reveals that sugarcane cultivation and conversion of bagasse to sugars contribute majorly to the global warming potential (Michailos, 2018).

2.6. Identified research gaps

Considering the insights derived from the review of literature and the need to develop a sustainable process for farnesene production using cyanobacterial cell factories, the subsequent research gaps were identified:

- The majority of research on farnesene production is focused on using host organisms, which requires heterotrophic carbon sources. Choosing autotrophic host organisms such as cyanobacteria, which utilize CO_2 as a carbon source, will be a sustainable method contributing towards a carbon-neutral economy.
- Since productivity is an important parameter for increased farnesene production. Cyanobacterial strains investigated so far have low farnesene productivity.
- Moreover, the cyanobacterial strains previously investigated have a doubling time of 4-5 h. Fast-growing cyanobacteria strain having a doubling time of 1.9-2 h will give increased farnesene productivity and hence the production. No systematic study of farnesene production using fast-growing cyanobacteria has been reported.
- The literature lacks the techno-economic analysis and life cycle assessment of farnesene production through engineered cyanobacteria using CO_2 as a carbon

source. This will provide the economic and environmental viability of the use of engineered cyanobacteria in the conceptual farnesene production plant.